LICENCE TO McMASTER UNIVERSITY

This _____Thesis_____ has been written
[Thesis, Project Report, etc.]

by _____Wendy Patricia Shoots_____ for
[Full Name(s)]
Undergraduate course number ___Geog 4C6___ at McMaster
University under the supervision/direction of _____
_____Dr. W.R. Rouse_____ .

In the interest of furthering teaching and research, I/we hereby grant to McMaster University:

1. The ownership of __1__ copy(ies) of this work;

2. A non-exclusive licence to make copies of this work, (or any part thereof) the copyright of which is vested in me/us, for the full term of the copyright, or for so long as may be legally permitted. Such copies shall only be made in response to a written request from the Library or any University or similar institution.

I/we further acknowledge that this work (or a surrogate copy thereof) may be consulted without restriction by any interested person.

_____   _Wendy Shoots_____
Signature of Witness,   **Signature of Student**
Supervisor

                    April 10, 1987
                         date

(This Licence to be bound with the work)

WATER DEPTH DETERMINATION

USING LANDSAT THEMATIC MAPPER DIGITAL IMAGERY

By

WENDY SHOOTS
8302495

A Research Paper

Submitted to the Department of Geography

in Fulfilment of the Requirements

of Geography 4C6

McMaster University

April 1987

ABSTRACT

An analysis was performed using Landsat 5 Thematic Mapper digital imagery to determine water depth of an area on the eastern coast of James Bay.

Classification methods, grouping water bodies into natural classes, were compared to established bathymetry of the area. Calculations for water depth were tried using a NASA sponsered water depth alogorithm developed by F.C. Polcyn.

The results of this study, presented graphically and tabularly, indicated the delineation bottom topography, but provided a range in digital pixel count values too small for proper determination of water depth.

It was concluded, that with few positive results, TM data is not a viable means of determining water depth in eastern James Bay.

ACKNOWLEDGEMENTS

TABLE OF CONTENTS

Page

LIST OF FIGURES

LIST OF PLATES

LIST OF TABLES

1. **INTRODUCTION**

In 1976 the International Hydrographic Bureau estimated that only 16% of the oceans of the world had sufficiently accurate soundings to determine sea floor topography (Kapoor, 1976). The history of shipping and navigation is filled with ship losses directly attributable to inaccurate depth information (Polcyn, 1973). But the hydrographic survey resources needed to chart the world's 360 million square kilometres of sea bed are limited. As a result much or the world's water bodies remain relatively unexplored and Canada is no exception. One of the more poorly mapped areas in the country is James Bay, despite the proximity of a major development project under construction. The most important piece of basic data needed is a detailed bathymetric map of James Bay (Meagher et al, 1976). James Bay, however, is a very large body of water with a very complex shoreline. Actual measurements of coastal water depths using ship-board techniques have proven to be extemely costly and time consuming. A faster, more cost efficient method of water depth determination, is therefore sought.

Remote sensing techniques have been used for a large variety of purposes. Their utilization has helped man to expand his understanding of the environment. This study examines the possibility of using remote sensing to accurately estimate coastal water depths for an area on the eastern coast of James Bay.

Landsat 5, the latest Landsat satellite, was launched in March of 1984. It is equipped with an experimental multispectral scanner known as the Thematic Mapper (TM). This new sensor system has improved spatial resolution of 30 m, added spectral coverage into the visible blue band and the thermal region of the electromagnetic spectrum, and increased radiometric sensitivity. These features, as well as Landsat's ability to cover the entire earth every 16 days, which allowing for quick updating, make Landsat a hopeful prospect in water depth determination.

1.2 APPROACH

TM allows sensing in the blue spectral band (0.45 to 0.52 um), and provides a greater facility for water penetration than previously available. Based on a TM scene which was taken in the vicinity of Paint Hills on the eastern coast of James Bay on August 17, 1985, two methods for determining water depth were tried and evaluated in this study. The first method involves a classification of the TM data into natural groups and comparing these classes to measured bathymetric data. The second method involves the use of a NASA sponsored water depth alogorithm developed by F.C. Polcyn (1976). The results of these methods are outlined and discussed in an attempt to reach some reasonable conclusion as to the feasability of using Landsat TM digital imagery as a method of water depth determination in James Bay.

2.   **PREVIOUS WORK**

Remote sensing of the water surface and of the ocean bed can be achieved by conventional aircraft and by satellite.   Airborne techniques have been carried out by a number of researchers: Brown et al., 1971; Jain et al., 1981; Weidmark et al., 1981; and O'Neill et al., 1985.   Although some of the results have been fairly good, with depth accuracies within 1.6 metres for 6 metre depths   (O'Neill et al., 1985), cost and time to collect imagery for the total water area would be excessive (Bullard, 1983).   Satellites, on the other hand, could theoretically provide complete coverage in a short time at comparitively low costs.

Satellite remote sensing was first used in a bathymetry experiment in 1975 by Polcyn and Lyzenga (1975) that employed the ERTS-1 satellite (now called Landsat 1).   Two channel processing, in the green and red portions of the visible spectrum, gave calculations up to 9 metres in depth with normal-gain Landsat data.   In 1976 a milestone experiment was carried out by F.C. Polcyn, along the Great Bahama Bank.   This experiment used high-gain Landsat MSS data which has a spectral coverage into the green band of the visible range ($0.5um$ - $0.6um$).   Measured parameters included water clarity, defined by attenuation coefficients, and bottom reflection.   Water depth was calculated using an alogorithm derived by Polcyn.   This equation, which includes the parameters that have an effect on the sun's energy as it passes through both air and water paths, and reflects from the ocean bottom, provided a relationship between signal voltage and the

depth of the water. With this alogorithm, depths to 22 metres were reliably measured at accuracies within 10% of measured values. P. Lohmann (1985) used this equation and a method of factor analysis on multispectral scanner data taken over the German Bight. He determined bottom profiles up to 10 metres in depth with a regression coefficient as high as 0.85. Tests to transfer the method to map water depths two dimensionally failed due to very strong variation of suspended material in that area, and the lack of recent bathymetric maps. In 1983 R.K. Bullard performed an experiment using Landsat digital imagery for an area of the Red Sea, along the Saudi Arabia coastline. By comparing classified pixel values to bathymetric contour maps, Bullard attempted to test the accuracy of depth determination. However, bathymetry maps were not reliable, and the presence of the tide influx also created some problems. Digital apparent radiance data from Landsat-1 were collected along the coastline of Nottawasaga Bay in southern Georgian Bay, for use in a study to detrermine coastal bathymetry (Bukata et al., 1976). The data were compared to existing hydrographic charts for areas with well - defined depth contours. The results of these comparisons revealed that Band-4 (0.5um - 0.6um) MSS data clearly delineated the bottom contours to a maximum penetration of about 14 metres, in coastal regions having very clear water conditions (ie. turbidity less than 1 FTU), (Bukata et al., 1976). All of the studies previously mentioned, used Landsat MSS data.

In 1976 an analysis was performed to determine the most useful spectral band for water-depth and bottom analysis to depths of 15 metres (Lyzenga et al., 1976). It was found that the optimum

sensing extended from (.45um to 0.55um).   This band, however, is not

covered by the Landsat MSS sensor, which has a spectral coverage

reaching only into the green band of the visible spectrum (0.5um -

0.6um). Thus, the Lyzenga study suggested a change in the positioning

of the Landsat MSS bands.   Bullard (1983) also noted the need for

greater spectral coverage.   He expressed an interest in the prospects

of a new multispectral scanning sensor called the Thematic Mapper

(TM),   This sensor was launched on Landsat 4 in 1982 and again on

Landsat 5 in 1984.   The Thematic Mapper has seven channels and an

increased spectral coverage into the blue band (0.45um - 0.52um) of

the visible spectrum.   In 1985, two studies were carried out using the

TM for determining coastal bathymetry.   H.H. Kim and G. Linebough

(1985) selected a small area adjacent to the South Cat Cay Island on

the northwestern section of the Great Bahama Bank.   The alogorithm

developed by Polcyn (1976) was used to process the image, but noting

the difficulty of obtaining the water leaving radiance as the depth

approaches zero (a variable in the equation), the researchers decided

instead, to derive the variable from a regression line which best fit

sounding points from a 1831 British survey, and the TM data.   A 0.95

correlation for 70 random points was determined. The ability to

establish an emperical relationship which could be used to generate

fairly accurate depth charts was thus demonstrated.   The second study

was carried out by Kim Richardson (1985), who used TM data for the

Island of Nantucket.   The Polcyn (1976) alogorithm was not used in

depth calculations in this study since specific parameters for the

equation were unobtainable.   Instead, comparisons were made to the

classified TM scene using nautical charts for Nantucket.   High visual

correlations were noted.

Landsat multispectral scanners,   especially   the   Thematic

Mapper   show great potentioal for becoming a viable means   of

determining coastal water depths.   This method,   if it can be proven

reliable, will save great amounts of time, energy and expense.

3.   **EXPERIMENTAL DESIGN**

3.1 STUDY SITE

In using remote bathymetry, the study site must meet certain specifications to be appropriate for the study.

    1) Water must be fairly clear
    2) There must be a minimum of cloud cover.
    3) There must be no ice cover.
    4) The sun elevation angle must be > 30°
    5) Control bathymetry measurements must be available.

The study area chosen is covered entirely by Paint Hills Field Sheet 3792.   This is an unpublished bathymetric map created by Environment Canada (1972), (Figure 2).

Paint Hills is located on the eastern coast of James Bay and covers a 30 kilometre stretch from latitude 52° 25' N to a latitude 53° 05'. The shoreline of this area is very irregular and highly indented.   It is an emerging coastline characterized by an abundance of large enclosed bays of irregular shapes.   The area is fairly low lying with low rocky hills and drumlin ridges forming the major relief.   The more resistant rock of the Paint Hill islands are the prominant relief in this area, with an elevation of 152 m above sea level.

The tides in eastern James Bay are semidiurnal with a moderate amplitude (Dohler, 1968; Godin, 1972, 1974). Mean and large tides are 1.46 and 2.1 m at Fort George, and 0.76 and 1.07 m at Eastmain (refer to Figure 1 for locations).
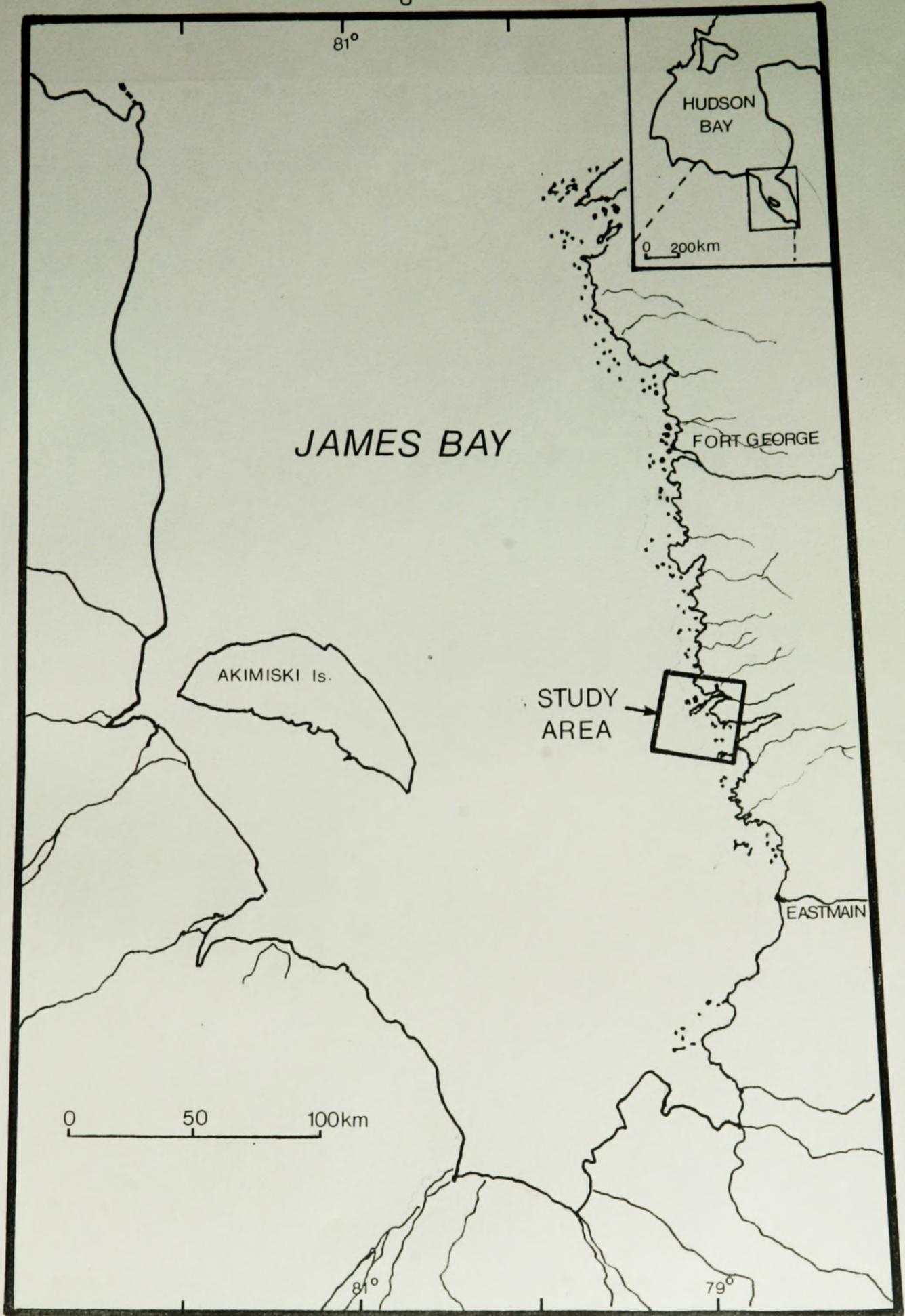
Figure 1:   James Bay.   Location Map showing the study site area.
            (Dionne, 1980)
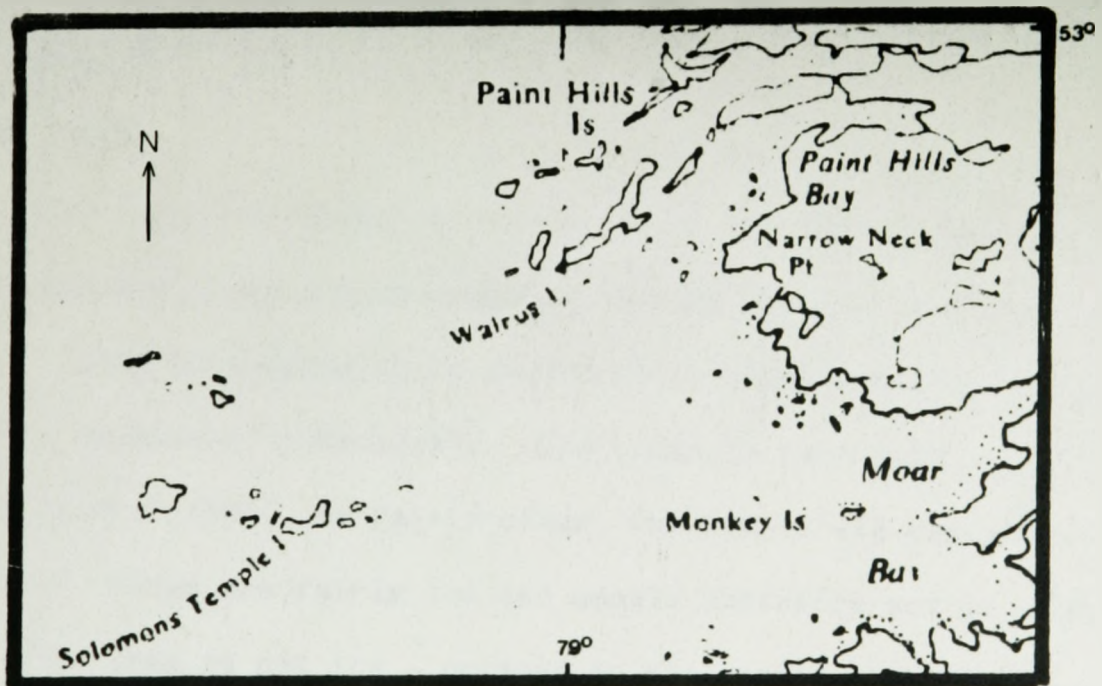
Figure 9A: Photograph of Field Sheet 3792: Paint Hills Bay, James Bay, N.W.T.; Department of the Environment (1972). Dotted lines are sounding tracks (depth soundings in metres). Figure 9B: is a location map of the same area, (from Meagher et al., 1976).

Tidal foreshore flats are found in most large embayments and around most offshore islands. They consist of a blanket of mud or fine sand usually less than 40 cm thick, overlying stratified grey silt and clay. The surface is strewn with thousands of boulders randomly distributed from the lowest to the highest levels (Dionne, 1980).

The seafloor is characterized by a rugged topography of high relief. The bottom is largely blanketed by Quaternary unconsolidated deposits with an average thickness of 10 m. Sediment samples taken by CALANUS (1959) and NARWHAL (1973), indicate a bottom type comprised quite consistently of mud, with 60% clay, 40% silt (Meagher et al. 1976).

James Bay is ice covered for eight of the twelve months, but remains generally ice free from mid August to the middle of October (US NAVY, 1968).

This area was chosen for a variety of reasons. Firstly, the area is generally shallow with depths ranging from 10 - 20 metres. Secondly, being so complex it is difficult to measure depths by other means (ie. shipboard techniques). The water in this area, according to Dionne (1981, 1986), is fairly clear, which will aid maximum light penetration. Tides are fairly low and should therefore not be a major factor. The area is not ice - covered in the summer, which is also the time that daytime solar altitude is assured to be greater than 30°. A Landsat image was available with only 10% cloud cover in August of 1985 and a bathymetric map (Field Sheet 3792) was available for an area within the image scene.

3.2 DATA ACQUISITION

Landsat TM data are recorded as an array of discrete picture elements, or pixels. A typical Landsat scene consists of 2300 lines and 3600 pixels. Reflected wavelengths from the earth's surface are recorded as a signal value for each pixel ranging from 0-255. This signal value is an average intensity value of the 30 m pixel surface. Landsat TM data is recorded in seven specific wavebands of the electromagnetic spectrum, each band having it's own usefulness. The three bands used in this study are:

Band 1: 0.45 - 0.52 um. Used for water body penetration, making it useful for coastal water mapping. It is also useful for differentiation of soil from vegetation and deciduous from coniferous flora.

Band 2: 0.52 - 0.60 um. Used to measure visible green reflectance peaks of vegetation for vigour assessment.

Band 4: 0.76 - 0.90 um. Useful for determining biomass content and for delineation of water bodies. (Source: CCRS Public Notice)

Landsat TM digital data are available from the Prince Albert Satellite Station in Saskatchewan on a computer compatible tape (CCT). Once the CCT tape has been received it may be entered into an Aries system such as the one located in the Methods and Design Area of the Faculty of Enviromental Studies at Waterloo University. This step transfers data from the tape to a disk. Figure 3 outlines this process. All analysis were carried out on the Aries system at Waterloo.

How remote sensing works

Landsat 5 is equipped with sensors for measuring radiation on the earth's surface. The information is converted into a signal which is beamed to a receiving station (A). There it is stored on magnetic tape, later to be processed by computer (B) and made into a coloured photographic image (C).

Antenna to relay satellite

Solar panels

Near-polar orbit

North Pole

700 km

Signal to ground

| X-ray | Ultraviolet | Visible | Infrared | Microwave | Radio |

Moosonee

185 km

Gatineau

Prince Albert

Earth's rotation
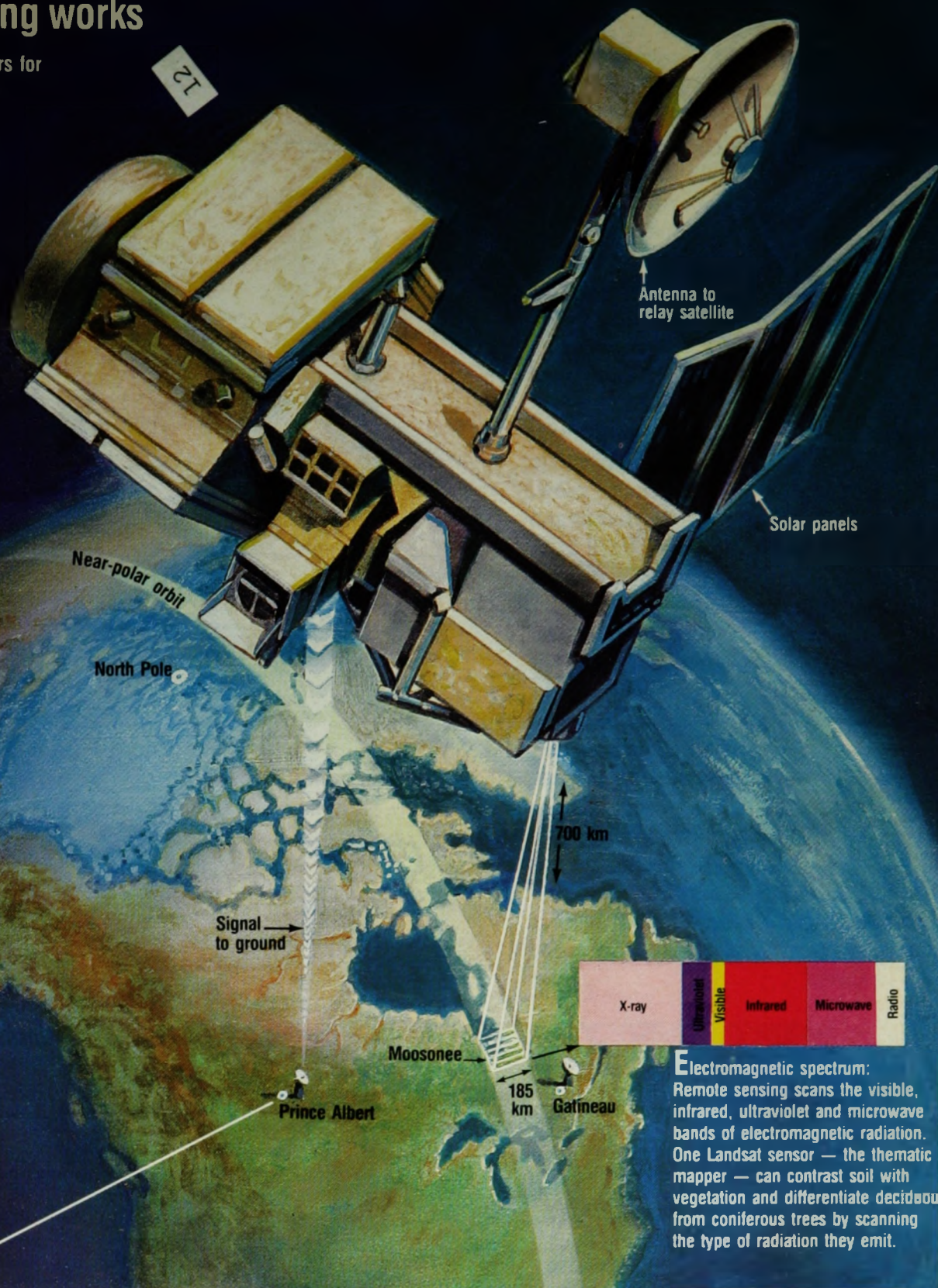
Electromagnetic spectrum: Remote sensing scans the visible, infrared, ultraviolet and microwave bands of electromagnetic radiation. One Landsat sensor — the thematic mapper — can contrast soil with vegetation and differentiate decidous from coniferous trees by scanning the type of radiation they emit.

A

B

C

James Bay

Moosonee
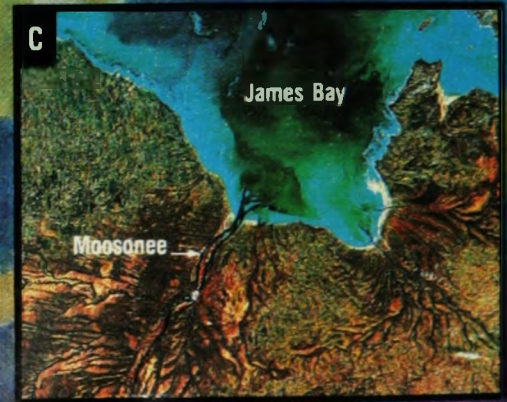
Canadian Geographic illustration by Don Macmillan

Figure 3: Landsat 5 - Data aquisition process.

The Landsat data for this analysis were obtained from a sub-area of Landsat 5 TM scene 50534-15430-50, path 20, row 23, quadrant 4.   This covers the area of Paint Hills in James Bay.   The sub-area consists of 851 lines and 1160 pixels per line, and covers an area of some 30 square kilometres.   The image date was 17AUG85 at 10:43 AM local time. The sun elevation for the image was 44°.   The image data were radiometrically raw and geometrically uncorrected. Since oceanic volume reflectance is contained in the lowest digital level of TM sensors, oceanographic applications require that a maximum amount of radiometric and geometric information be preserved during processing. Therefore, geometric corrections are carried out by the user.

3.3   IMAGE PROCESSING

3.3.1 Image Display

Once the data are in disk form they are available to the user. The data may be displayed in image form upon a colour screen if data from 3 different wavebands are used. TM band 1, 2, and 4 were chosen. Bands 1 and 2 give water depth penetration and band 4 delineates clearly the shoreline.   Plates 1 and 2 show the displayed image. Most of the work carried out on the data set, pertain to band 1 since this band gives the best water penetration.

14

Plate 1: Image display on the Waterloo Aries system.

Plate 2: Displayed image - Paint Hills Bay (TM Bands 1, 2, and 4)

3.3.2 Geometric Correction

To rectify distortions which are imposed on Landsat imagery when it is being recorded, a geometric correction must be performed. Using a computer program in the Waterloo Aries II computer system, the image was mechanically stretched to fit over a regular Universal Transverse Mercator (UTM) grid. In this way raw data are corrected for linear drifts and offsets which are inherent errors in the inertial system. Using Field Sheet 3792, precise UTM coordinates (northings and eastings) could be obtained for points on the image. Reference points, such as islands and bays, were identified with the aid of a graphic cursor on the diplayed image. A polynomial equation transformed line and pixel image coordinates to UTM map indices. The image was resampled and a new geometrically correct image was created. The corrected image had a conversion of 30 lines per 2500 metre northings, and 30 pixels per 2500 metre eastings.

3.4 CLASSIFICATION

Classification is the assignment of all of the various reflectance patterns found on the image to distinguishable ground cover types. There are two approaches commonly used in image processing to identify natural groups: supervised and unsupervised classification.

3.4.1 Supervised Classification

In this study, a supervised classification was carried out to include all water bodies. This step required that training areas for water be drawn on the image with the cursor and entered into the computer. Foreshore flats and small inland lakes were included in the training area so that all water would be classified. Approximately 15 training segments were entered to make up the water body training area. Plate 3 shows the classified image, all water being shown in red.

3.4.2 Unsupervised Classification

An unsupervised classification was then carried out on the newly generated water class. An unsupervised classification refers to a procedure using the Maximum Likelihood Classification alogorithm such that all pixels are grouped by the probability of their occurance within a class. No direct interaction with the image is necessary for this classification. Using this process, a seven class theme file was generated (refer to Plate 4).
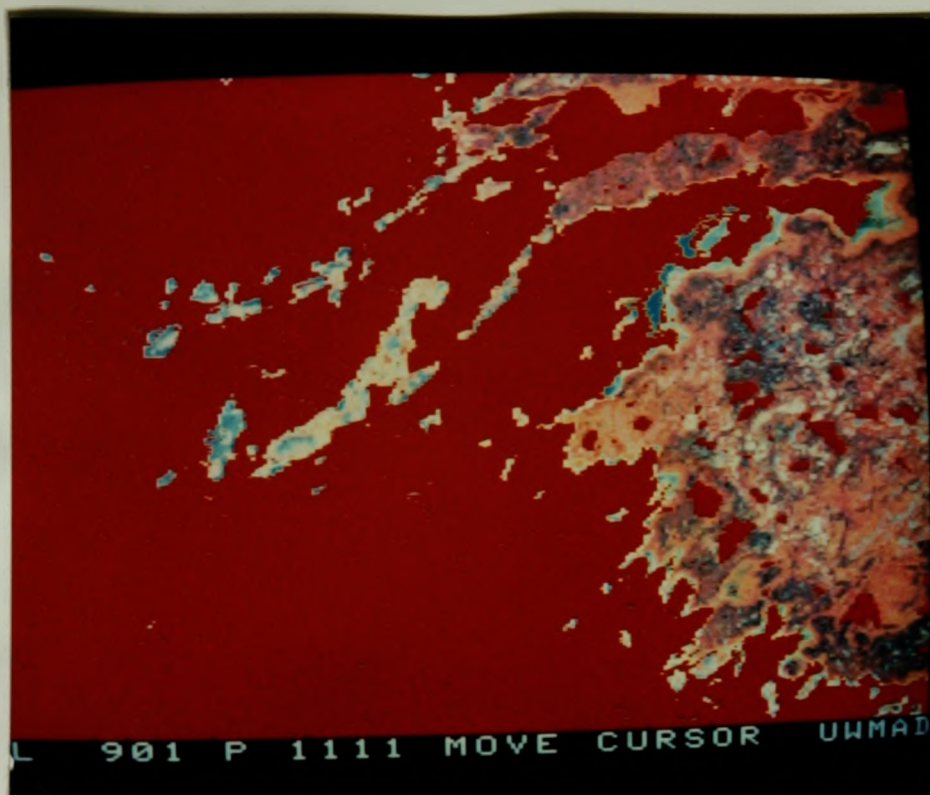
Plate 3: Supervised classification of water.
The red areas represent the water class.
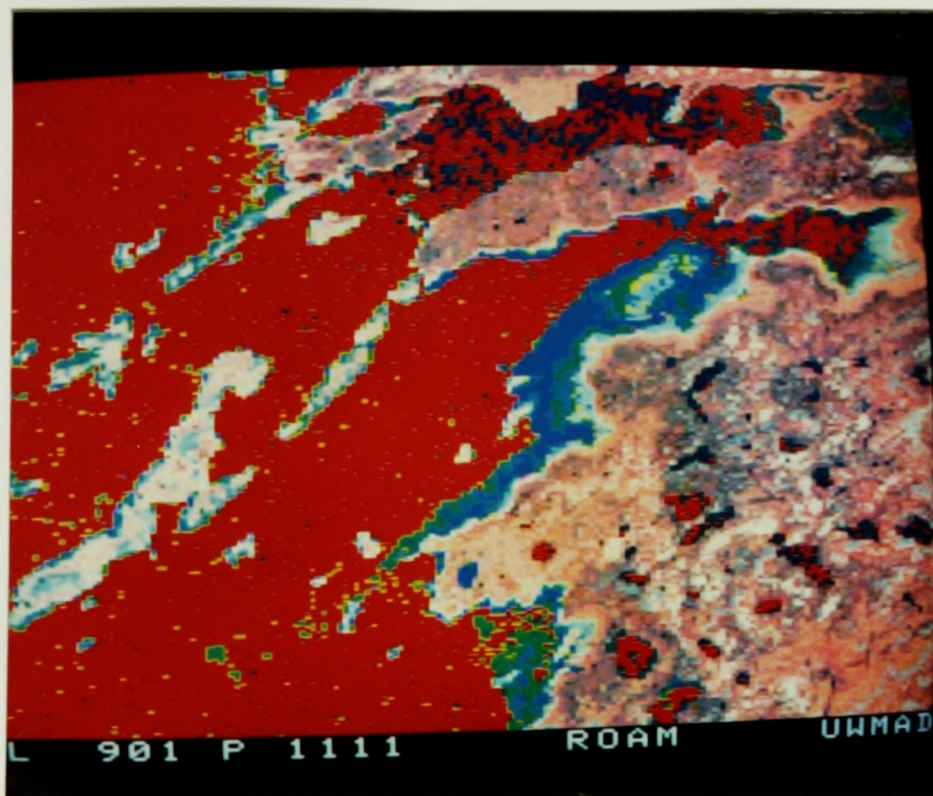
Plate 4: Unsupervised classification of water.
Seven classes are represented.

3.5 WATER DEPTH DETERMINATION

Remote bathymetry takes advantage of two characteristics. Water selectively absorbs different wavelengths of light, and energy at each wavelength is strongly absorbed as a function of the depth of the water. As the sun's energy penetrates the ocean, losses occur (1) at the surface, (2) through the water column, (3) at the reflection from the bottom, then (4) through the water column for the return path, (5) at the surface again, and finally (6) through the atmosphere to the satellite where it is collected by multispectral scanners (TM) in selected wavelength bands. Figure 4 illustrates this process.

The Polcyn model (1976) develops a relationship between signal voltage from the Landsat TM and the depth of the water which includes the parameters that have an effect on the sun's energy as it passes through both the air and water paths and reflects from the ocean bottom (Polcyn, 1976). Due to the complexity of the variables in this situation, Polcyn assumes three simplifying assumptions: (1) neglect scattering in the water, (2) assume that sensor signals come only from direct solar radiation defined as $K\!\downarrow\!o$ and (3) assume the water attenuation coefficient is independent of radiance distribution. Given these assumptions the Polcyn model can be expressed by the equation:

$$V = Vs + Vo \, e^{-2za} \qquad\qquad (1)$$

so,

$$z = \frac{-1}{2a} \, \ln \frac{Vi - Vs}{Vo} \qquad\qquad (2)$$

where,

Vi = the water leaving radiance from depth i

Vs = the water leaving radiance received from an area of infinite depth (no bottom reflectance)

α = irradiance attenuation coefficient (m^{-1})

z = water depth (m)

Vo = water leaving radiance as the depth approaches zero.

Vo is given by the equation:

$$Vo = ks \frac{T1\ T2}{n^2} K{\downarrow}o\ T\ \frac{rb}{\pi} \qquad (3)$$

where,

ks = Landsat 5 TM 1 sensitivity constant

T1 T2 = water surface transmittance (.98)

n = index of refraction (1.33)

$K{\downarrow}o$ = surface irradiance at time of satellite passing in the blue waveband ($mw\ cm^{-1}$)

T = e^{-t} where t = extinction coefficient (found in Guttman tables)

rb = bottom reflectance

Hence, if Vo and α are known or can be assumed, z can be computed by inspecting the Landsat signals after first subtracting the mean deep water signal (Vs).
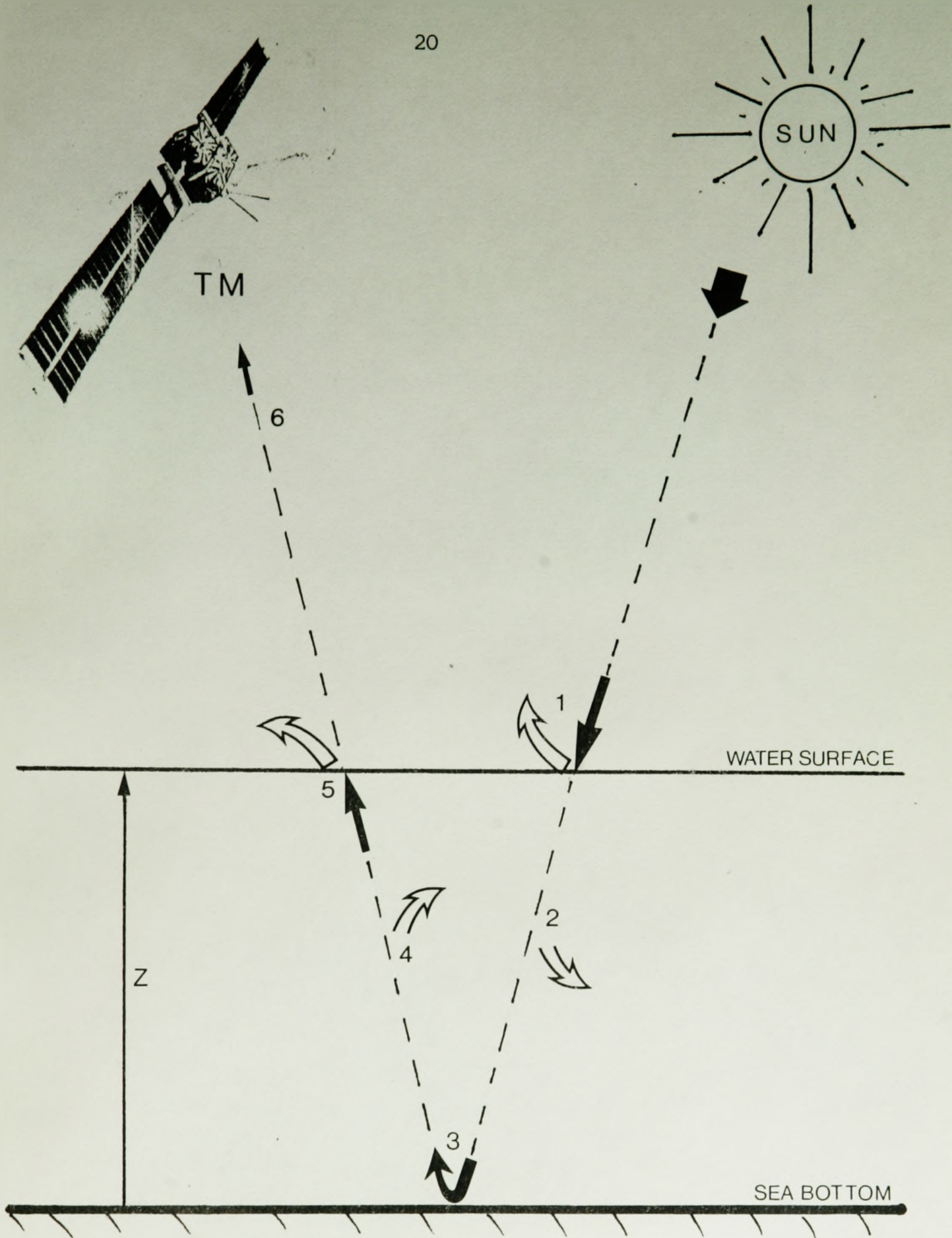
Figure 4: Penetration of the sun's energy into a water body.

(Vs) The deep water signal:

Vs was determined by taking an average pixel value for known deep water. With reference to Field Sheet 3792 points at which depths were greater than 40 metres were marked out by the cursor. The pixel values given ranged between 50 and 53. The average value was a count of 51.

(a) The attenuation coefficient:

The attenuation coefficient is a measure of water clarity, or the amount of light scattered or absorbed in a specific wavelength through the water column. Polcyn (1976) used surface measurements by a photometer to calculate attenuation coefficients for specific study sites. Since measurements are not possible in this study, an attenuation coefficeient must be estimated. Smith and Baker (1978) list spectral attenuation coefficients for various wavelengths (see Appendix 1, Table 1). Attenuation coefficients can vary depending on suspended sediments in the water and chlorophyll like pigments. An average attenuation coefficient was calculated for the spectral range from (0.45 - 0.52um), corresponding to TM band-1. Diffuse attenuation for clear water was found to be 0.0283 m^{-1}. Attenuation coefficient not attributable to chlorophyll pigments was averaged out to 0.089 m^{-1} and a coefficient of 0.121m^{-1} was assigned to attenuation due to chlorophyll like pigments. Possible attenuation coefficients, therefore, are as follows:

1) for clear water = 0.0283 m^{-1}
2) for water without chlorophyll = 0.0283 + 0.089 = 0.117 m^{-1}
3) for water with chlorophyll = 0.0283 + 0.121 = 0.149 m^{-1}

(Vo) Signal as depth approaches zero:

Most of the terms in Vo are constants or known parameters. The Landsat sensitivity constant (ks) was obtained through the Canada Centre for Remote Sensing (CCRS), and is defined as the saturation count, 255, divided by the TM spectral radiance range, 1.536 mw/cm^{2}sr^{-1} giving a TM band 1 sensitivity constant of 166.

The surface irradiance (K↓o) at the time of the satellite passing was estimated for the blue band using a computer model developed by B. McArthur of the Atmospheric Environmental Service (AES). At a local apparent time of 10:38 a.m., on August 17, 1985, the model estimated a value of 9.485 mw cm$_{-2}$.

The spectral transmittance (T) was estimated from Guttman tables for the blue waveband (0.45 - 0.52 um.). The value determined was 0.93 (Guttman, 1968).

Finally, the bottom reflectance was estimated for an assumed mud bottom type (Meagher et al., 1976). Though albedo values for mud bottoms are not readily available, it has been found that most surfaces, with the exception of sand, have less than 10% reflectancy in the blue band of the visible spectrum (Paltridge and Platt, 1976), (see Appendix 1, Figure 1). A study by Weidmark et al., (1981) determined passive bathymetric measurements in the Bruce Peninsula and used an albedo value of 0.09 for a mud bottom type. It would seem reasonable then, that reflectance values below 10% would be appropriate for this study.

3.6   DATA ANALYSIS

3.6.1   Water Depth Processing

A program, "WATERDEPTH", that used the Polcyn alogorithm to generate water depths for individual line/pixel values, was created by J. Piwowar of the University of Waterloo. This program could also generate water depth images which included all line/pixel values.

Fifty samples were randomly chosen from Field Sheet 3792 by arbitrarily throwing a pencil upon the map and recording the depth value at the lead point. The UTM northing and easting coordinates for this point were then recorded and subsequently converted to line and pixel values.

These samples could then be entered into the Waterloo computer to generate calculated water depth values. The program allows the user to alter parameters within the Polcyn model using equation (2). In this way different values could be entered for site specific parameters to show how these parameters may affect the resulting depths. Of the given values in equation (2) only three are site specific and therefore not constants. These are the attenuation coefficient (α), the bottom reflectance (rb), and the deep water pixel values (Vs).

Since James Bay is a fairly cold environment it is unlikely that chlorophyll particles would be prominent in the water. For this reason it was felt that 0.117 m^{-1}, the attenuation value for particles not due to chlorophyll, would be a good estimate of the attenuation coefficient in James Bay. It can also be said with confidence that the water in this area is not completely pure, or clear, sea water.

However, Dionne (1980, 1986), points out that the shoreline on the northeast part of James Bay is comprised of outcrops of Precambrian rock which is not susceptible to erosion. Therefore, he notes, that although some erosion of various till deposits along the shoreline might occur, it is relatively small, hence the water is comparatively free of suspended sediment. For this reason a second attenuation coefficient was considered -- An attenuation value was taken that fell between pure water (0.0283 m^{-1}) and water with attenuation due to both chlorophyll and other particles (0.149 m^{-1}). This gave a value of 0.086 m^{-1}, which considers water to be a little clearer than the above-mentioned value of 0.117 m^{-1}.

The deep water pixel value (Vs), as noted earlier, was found to give an average count value of 51. However, to see how sensitive this value was in the Polcyn model, counts of 50 and 52 were also tried.

Bottom reflectancy (rb) as previously noted was assumed to be less than 0.10. Since this value is very subjective, it was decided to also test values 0.025, 0.05, 0.075 and 0.09.

For added clarification, one trial was run for an attenuation coefficient of 0.149 m^{-1}, and one trial was run for a deep water count of 53. The trial sequence and the various parameters used are outlined in Table 1.

Correlation tests were performed on the data using the statistical computing system, MINITAB. Calculated water depths were correlated against the actual measured depths from Field Sheet 3792.

TABLE 1

TRIAL SEQUENCE FOR CHOSEN PARAMETERS

α=attenuation coefficient (m^{-1}), Vs=deep water pixel count

rb=bottom reflectance, and r^2=correlation coefficient

TRIAL	α	Vs	rb
1	.117	50	.025
2	.117	51	.025
3	.117	52	.025
4	.117	50	.05
5	.117	51	.05
6	.117	52	.05
7	.117	50	.075
8	.117	51	.075
9	.117	52	.075
10	.117	50	.09
11	.117	51	.09
12	.117	52	.09
13	.086	50	.025
14	.086	51	.025
15	.086	52	.025
16	.086	50	.05
17	.086	51	.05
18	.086	52	.05
19	.086	50	.075
20	.086	51	.075
21	.086	52	.075
22	.086	50	.09
23	.086	51	.09
24	.086	52	.09
25	.149	52	.05
26	.086	53	.05

3.6.2 Water Depth Image

The second option of the program generates an overall water depth image.   Four such images were created somewhat randomly,   since correlation tests had not yet been carried out on the data, and it was difficult to tell which would have the best results.   The four images were created using the same parameters as used in trials 6, 8, 21, and 26. These images are shown in Plates 5-10.
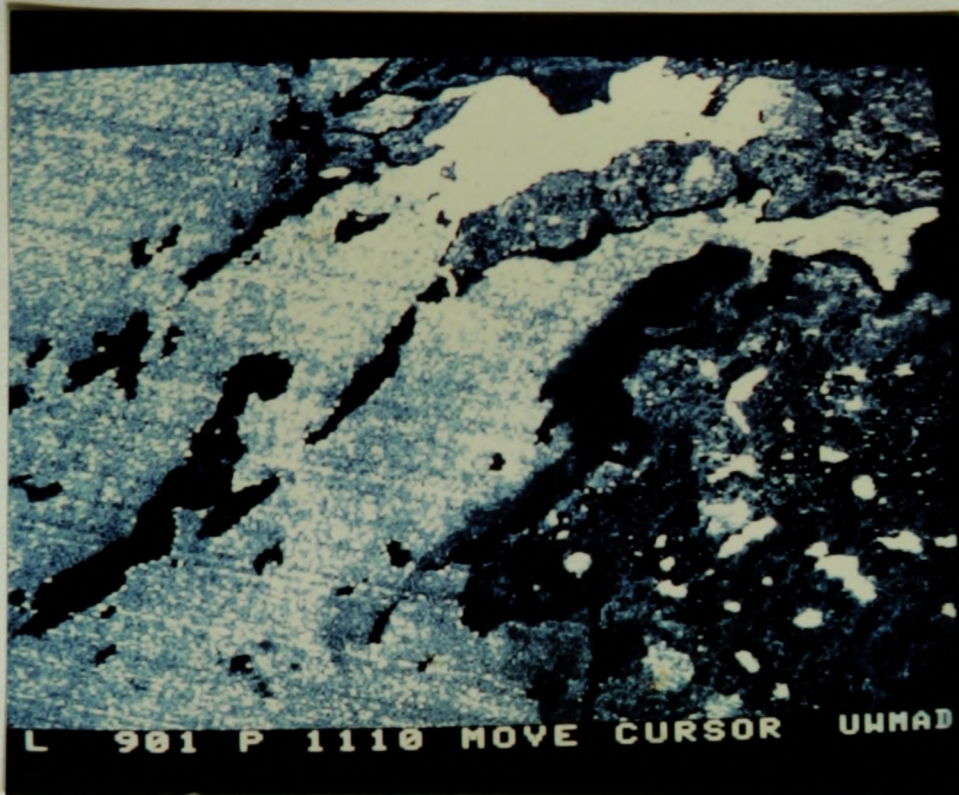
Plate 5: Calculated water depth image of Paint
          Hills Bay for Trial 6.

Plate 6: Calculated water depth image of
          Paint Hills Bay for Trial 8.
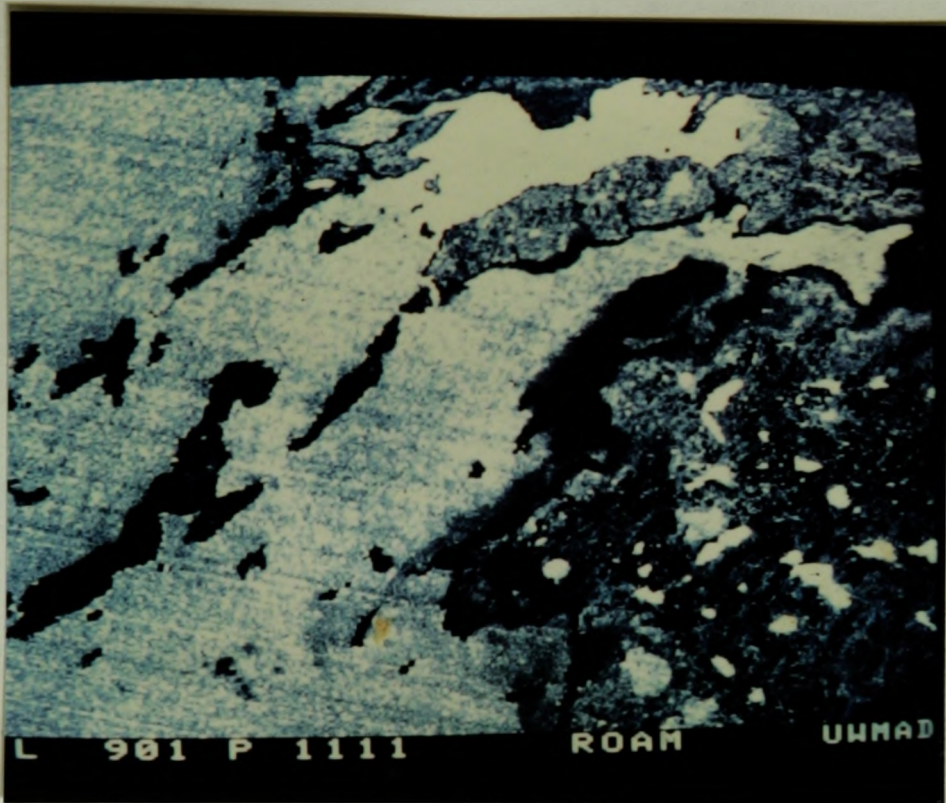
Plate 7:   Calculated water depth image of
           Paint Hills Bay for Trial 21.
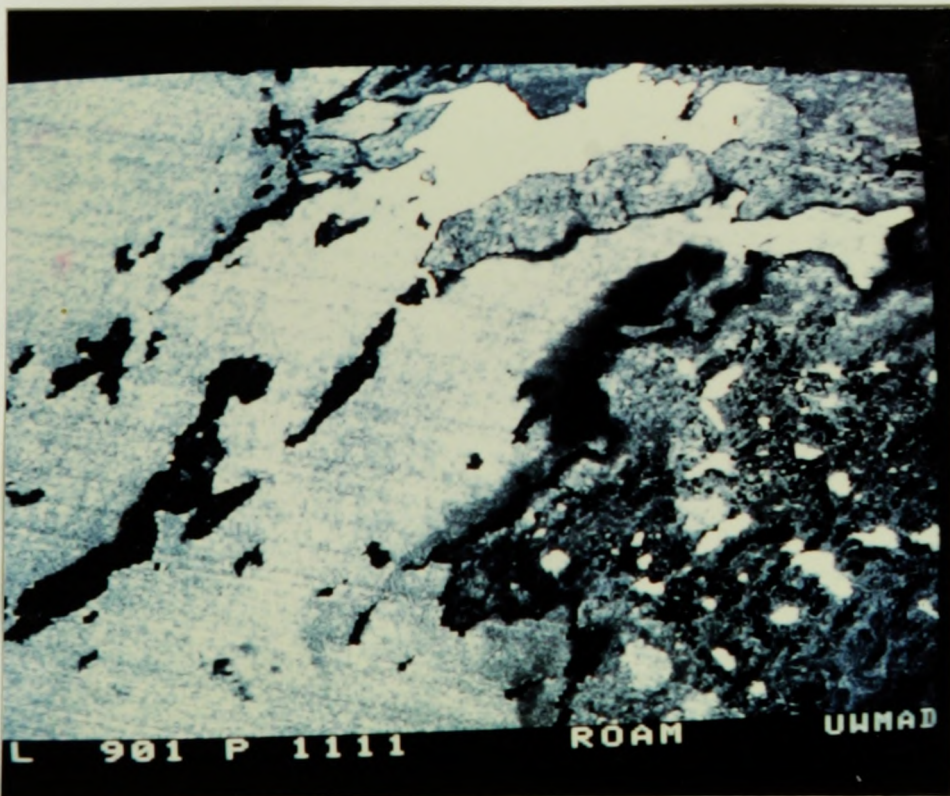
Plate 8:   Calculated water depth image of
           Paint Hills Bay for Trial 26.

4.   **RESULTS**

4.1 CLASSIFICATION

Seven   classes   were   generated   by   the   unsupervised
classification of the water body.   However, 95% of the pixel values
fell into class 1.   A histogram for TM band 1 data (Figure 5) reveals
a very small range in pixel values, with almost all of the data
falling between the digital counts of 50 and 60.   Therefore, the main
water body, unfortunately, did not provide a large enough range to
create more than one class.   As a result, only the foreshore flats
were classified.   This is shown clearly in Plate 4, where the red area
represents class 1 and the rest of the colour designated areas make up
the remaining 6 classes.   As a result, no comparisons to measured
bathymetric trends could be applied.

4.2 WATER DEPTH CALCULATIONS RESULTS

Table 3 lists the measured water depths for the entire sample
set.   Table 2 lists the calculated water depths for each   trial,   for
each pixel value found within the sample set.   The mean values of both
these tables are graphed in Figure 6.   From this graph it is apparent
that calculated water depths decrease with increasing pixel count
values.   For example, one might expect shallower water depths at
pixel values of 58 than at pixel count values of 54.

30


```
***              HISTOGRAM SUMMARY              ***

FEATURE FILE NAME :                                    GCIFFTM01
HISTOGRAM RANGE                                        0 TO 255
NUMBER OF BINS IN HISTOGRAM :                          256
BIN SIZE FOR HISTOGRAM                                 1
TOTAL NUMBER OF POINTS READ FROM FEATURE FILE :        987160
NUMBER OF POINTS THAT OVERFLOWED :                     0
PERCENTAGE OF POINTS THAT OVERFLOWED :                 0.00
NUMBER OF POINTS IN HISTOGRAM :                        987160
PERCENTAGE OF POINTS IN HISTOGRAM :                    100.00
FIRST NON-ZERO VALUE :                                 0
LAST NON-ZERO VALUE :                                  215
MEAN OF VALUES IN HISTOGRAM :                          48.12
STANDARD DEVIATION OF VALUES IN HISTOGRAM :            20.40

*** HEADER BLOCK STATISTICS HAVE BEEN UPDATED
```

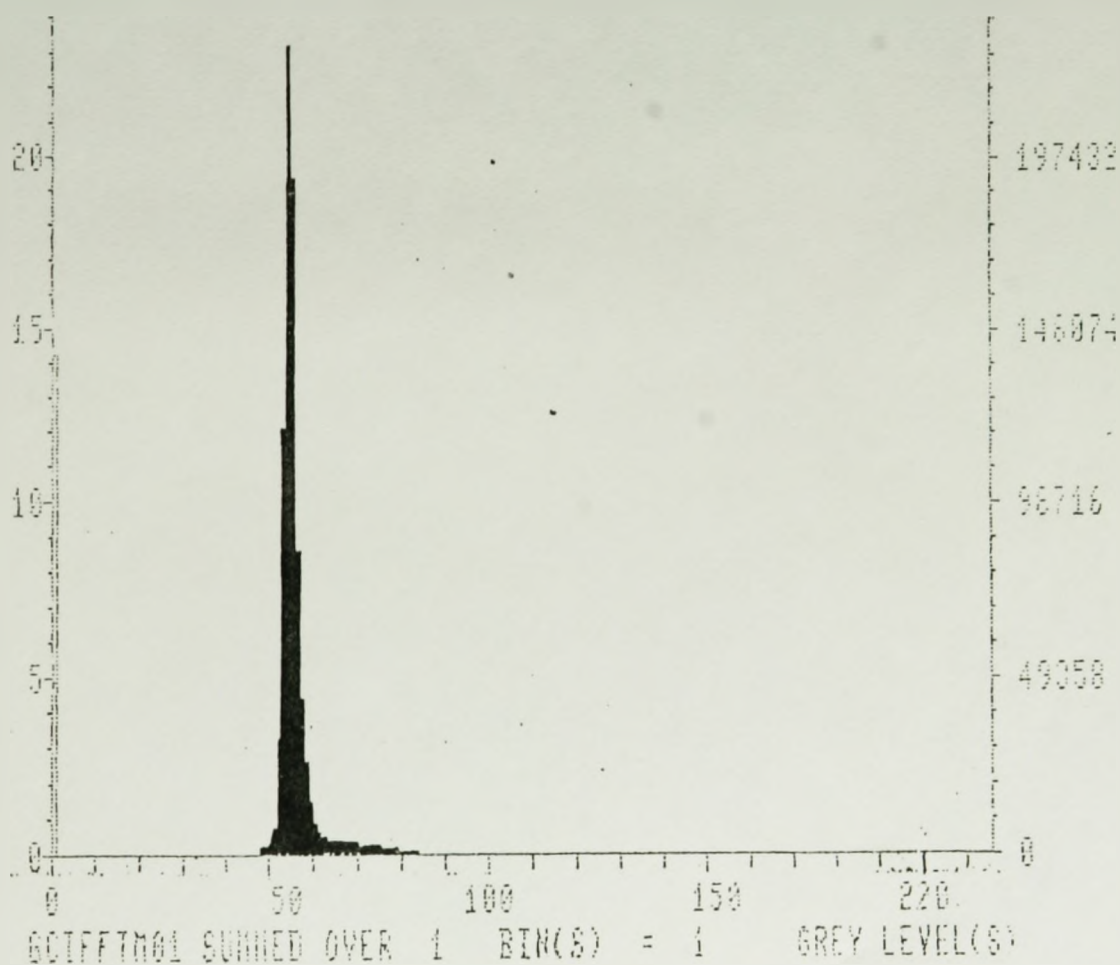Figure 5: Histogram of TM band 1 data showing all pixel counts
within the image falling between 48 and 83.

TABLE 2

CALCULATED WATER DEPTHS
FOR DIGITAL COUNTS OF EACH TRIAL

Water Depths in metres

COUNT	50	52	53	54	55	56	57	58	60	77	81
TRIAL #											
1	0.0	5.01	3.28	2.05	1.09	0.31	-0.35	-0.92	-1.87	-6.12	-6.71
	0.0	7.97	5.01	3.28	2.05	1.09	0.31	-0.35	-1.42	-5.45	-6.56
3	0.0	0.0	7.97	5.01	3.28	2.05	1.09	0.31	-0.92	-5.79	-6.42
4	0.0	7.97	6.24	5.01	4.05	3.28	2.61	2.05	1.09	-3.15	-3.74
5	0.0	10.95	7.97	6.24	5.01	4.05	3.28	2.61	1.54	-2.99	-3.60
6	0.0	0.0	10.93	7.97	6.24	5.01	4.05	3.28	2.05	-2.86	-3.46
7	0.0	9.70	7.97	6.74	5.79	5.01	4.35	3.78	2.83	-1.42	-2.01
8	0.0	12.67	9.70	7.97	6.74	5.79	5.01	4.35	3.28	-1.26	-1.87
9	0.0	0.0	12.67	9.70	7.97	6.74	5.79	5.01	3.78	-1.09	-1.73
10	0.0	10.48	8.75	7.52	6.57	5.79	5.13	4.56	3.60	-0.64	-1.23
11	0.0	13.44	10.48	8.75	7.52	6.57	5.79	5.13	4.04	-0.48	-1.09
12	0.0	0.0	13.44	10.48	8.75	7.52	6.57	5.79	4.56	-0.31	-0.95
13	0.0	6.81	4.46	2.78	1.49	0.49	-0.47	-1.25	-2.54	-8.32	-9.12
14	0.0	10.84	6.81	4.46	2.78	1.49	0.43	-0.47	-1.93	-8.10	-8.93
15	0.0	0.0	10.84	6.81	4.46	2.78	1.49	0.43	-1.25	-7.87	-8.74
16	0.0	10.84	8.49	6.81	5.52	4.46	3.56	2.78	1.49	-4.29	-5.09
17	0.0	14.87	10.84	8.49	6.81	5.52	4.46	3.56	2.10	-4.07	-4.90
18	0.0	0.0	14.87	10.84	8.49	6.81	5.52	4.46	2.78	-3.84	-4.71
19	0.0	13.20	10.84	9.17	7.87	6.18	5.92	5.14	3.84	-1.93	-2.74
20	0.0	17.23	13.20	10.84	9.17	7.87	6.18	5.92	4.63	-1.70	-2.56
21	0.0	0.0	17.23	13.20	10.84	9.17	7.87	6.18	5.14	-1.48	-2.35
22	0.0	11.90	11.90	10.23	8.93	7.81	7.0	6.2	4.9	-0.87	-1.67
23	0.0	18.29	14.26	11.90	10.23	8.93	7.87	6.98	5.52	-0.65	-1.48
24	0.0	0.0	18.23	14.26	11.90	10.23	8.93	7.87	6.20	-0.42	-1.29
25	0.0	0.0	8.58	6.26	4.90	3.93	3.18	2.57	1.60	-2.23	-2.72
26	0.0	0.0	0.0	14.87	10.84	8.49	6.81	5.52	3.56	-3.60	-4.50
MEAN	0.0	11.13	9.67	8.27	6.51	5.28	4.37	3.52	2.16	-3.14	-3.87
RANGE	0.0	18.29	18.23	12.82	10.81	9.92	9.28	9.12	8.74	8.01	8.13
ST.DEV	0.0	3.19	4.22	3.40	2.99	2.78	2.55	2.59	2.55	2.53	2.89

TABLE 3

MEASEURED WATER DEPTHS FOR

FIFTY SAMPLE POINTS

Water depths in metres

| NORTHING	EASTING	LINE	PIXEL	COUNT	MEASURED DEPTH
5862100	637800	1264	1261	55	9.6
5866000	638100	1134	1271	53	10.4
5866250	640650	1126	1356	54	6.6
5865150	640000	1162	1334	54	8.2
5867000	634900	1101	1164	55	9.6
5858900	622650	1371	756	54	25.0
5858550	636900	1383	1231	53	13.6
5866000	635350	1134	.1179	54	19.0
5864950	637600	1169	1254	54	2.2
5859400	638500	1354	1284	54	14.2
5863850	638100	1206	1271	54	8.4
5872750	643850	1151	1463	56	10.0
5870700	641300	978	1378	53	5.6
5862200	637500	1261	1251	56	8.8
5867300	633650	1091	1123	77	17.8
5865500	637450	1151	1249	52	2.0
5866450	639300	1119	1311	53	3.6
5862900	631050	1238	1036	54	19.8
5866300	636050	1124	1203	54	18.2
5866950	641650	1103	1389	53	3.6
5853400	618700	1554	1125	54	7.4
5872000	643650	934	1456	50	2.6
5867100	634600	1098	1145	55	16.0
5867150	639000	1096	1301	60	5.2
5866000	634300	1134	1144	55	4.6
5865400	638750	1154	1293	55	17.0
5862000	638050	1268	1269	55	12.4
5861250	633000	1293	1101	56	20.4
5859750	638200	1343	1274	55	13.6
5857950	635350	1403	1179	54	23.6
5863700	638500	1211	1284	55	9.4
5861950	636550	1269	1219	54	10.0
5861900	638250	1271	1276	54	11.8
5869750	640450	1009	1349	81	2.4
5861500	636200	1284	1208	54	13.6
5864950	639500	1169	1318	57	6.8
5861950	635256	1269	1176	54	16.4
5865250	639800	1159	1328	55	8.4
5865800	639250	1141	1309	55	8.8
5864850	639050	1173	1303	56	11.0
5862450	637850	1253	1263	56	10.4
5862550	635050	1249	1169	53	15.6
5865350	639050	1156	1303	53	5.6
5862450	634950	1253	1166	55	17.4
5862700	631850	1244	1063	54	20.6
5865600	635400	1148	1181	58	14.2
5863750	639050	1209	1303	57	5.8
5861950	640600	1269	1354	56	11.2
5866190	631440	1126	1049	53	4.6
5865080	635446	1165	1183	58	3.6
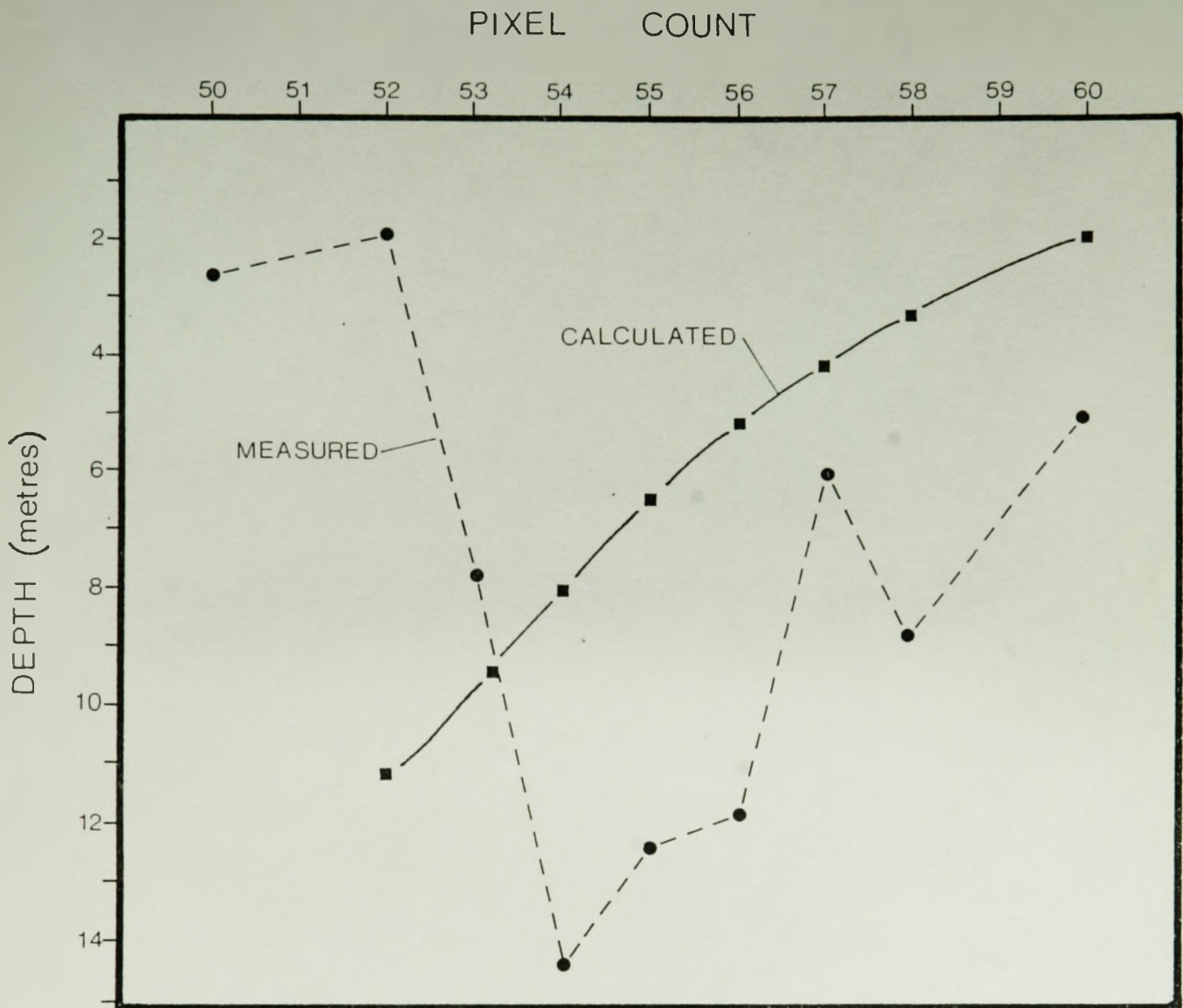
Figure 6: Mean water depth values for both measured and calculated water depths for the sample set.

Figure 7 is a graph showing the ranges in measured depths for the various digital counts within the data set. This graph reveals a large range in depths for any particular pixel value.

Correlations of calculated depths to the measured depths are given in Table 4, which lists all of the correlation values (r^2) for each trial. None of the correlations proved to be significant. However, some general trends can be noted. Figure 8 shows graphically the correlations. From this graph it is apparent that both bottom reflectancy and the deep water pixel values affect the correlations. Changes in the attenuation coefficient do not seem to have a great effect, shown by the closeness of the lines. The correlation values do increase somewhat with increasing bottom reflectancy. This might be expected, since increased relectancy should create deeper depth penetration. The correlation values also increase with increased deep water pixel counts. In fact, the best correlation (0.44), was obtained when a deep water pixel count of 53 was used. This does not make alot of sense since higher pixel values should correspond with less water penetration.

4.3 WATER DEPTH IMAGERY RESULTS

The water depth images, shown in Plates 5-8, show an area which can be compared to the measured bathymetry (Figure 9). In these plates the light areas should be areas of deeper water while darker areas should be shallow water or land. This however, is definitely not the case. The light areas instead, are showing up along the
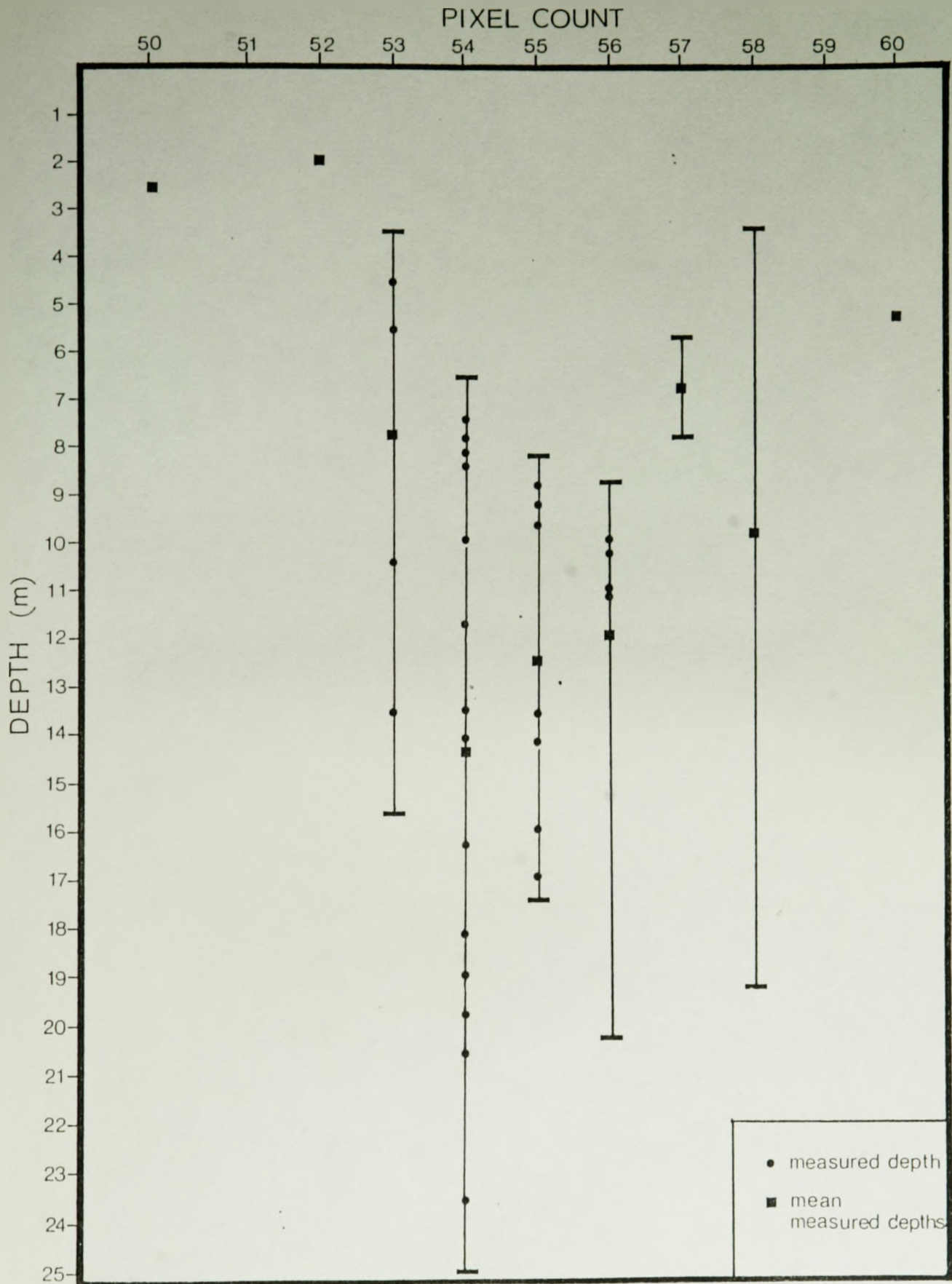
Figure 7: Ranges in measured depths for the corresponding
pixel counts in the sample.

TABLE 4

CORRELATION COEFFICIENTS
OF CALCULATED TRAIL DEPTHS AGAINST MEASURED DEPTHS

a =attenuation coefficient (m^{-1}), Vs=deep water pixel count

rb=bottom reflectance, and r^2=correlation coefficient

| TRIAL	α	Vs	rb	r^2
1	.117	50	.025	0.031
2	.117	51	.025	-0.002
3	.117	52	.025	0.124
4	.117	50	.05	0.069
5	.117	51	.05	0.047
6	.117	52	.05	0.143
7	.117	50	.075	0.091
8	.117	51	.075	0.065
9	.117	52	.075	0.176
10	.117	50	.09	0.093
11	.117	51	.09	0.071
12	.117	52	.09	0.186
13	.086	50	.025	0.008
14	.086	51	.025	0.015
15	.086	52	.025	0.106
16	.086	50	.05	0.069
17	.086	51	.05	0.047
18	.086	52	.05	0.155
19	.086	50	.075	0.089
20	.086	51	.075	0.063
21	.086	52	.075	0.180
22	.086	50	.09	0.101
23	.086	51	.09	0.071
24	.086	52	.09	0.187
25	.149	52	.05	0.154
26	.086	53	.05	0.441
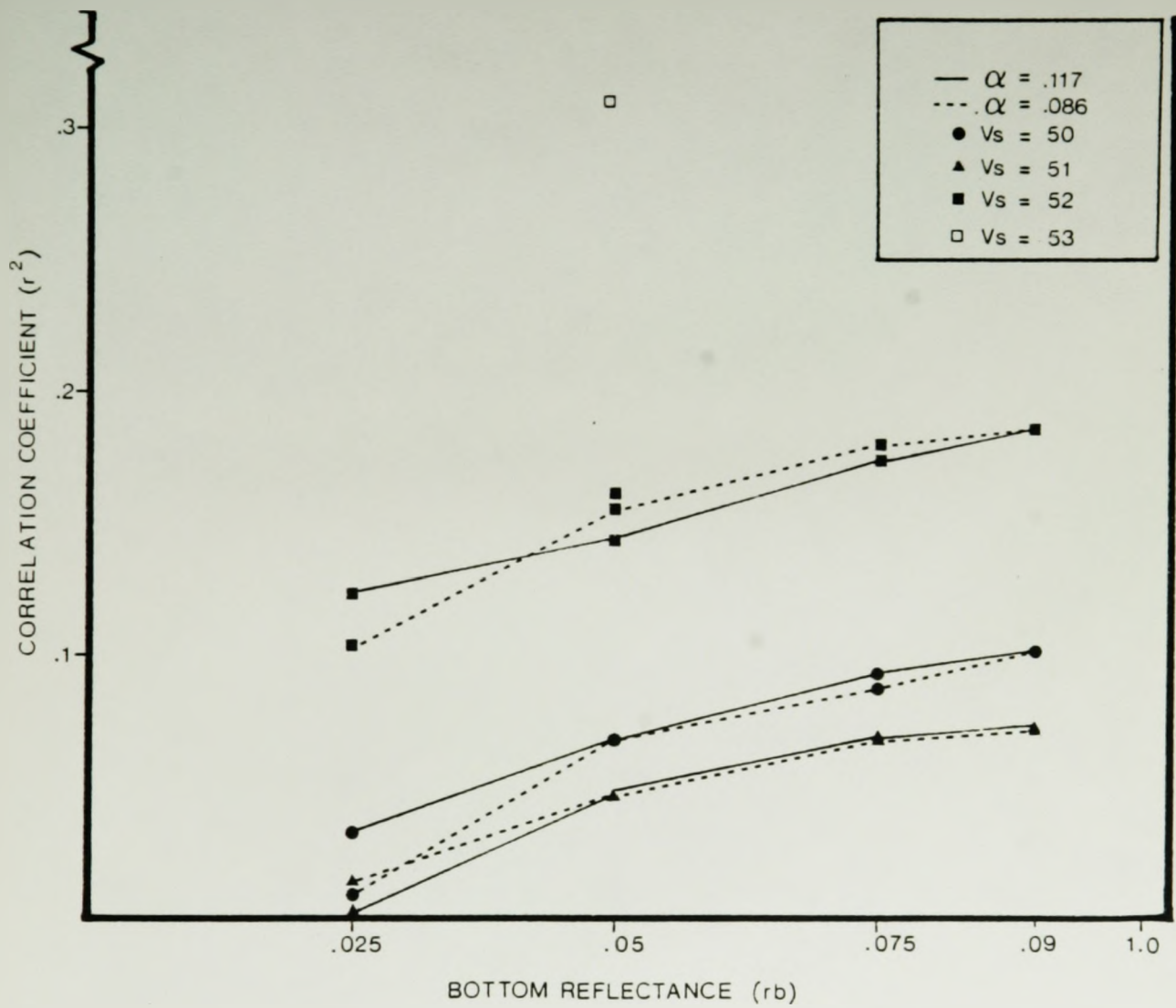
Figure 8: Correlation coefficients for all combinations of bottom reflectance (rb), deep water pixel values (Vs), and attenuation coefficients (α) used in the trial set.
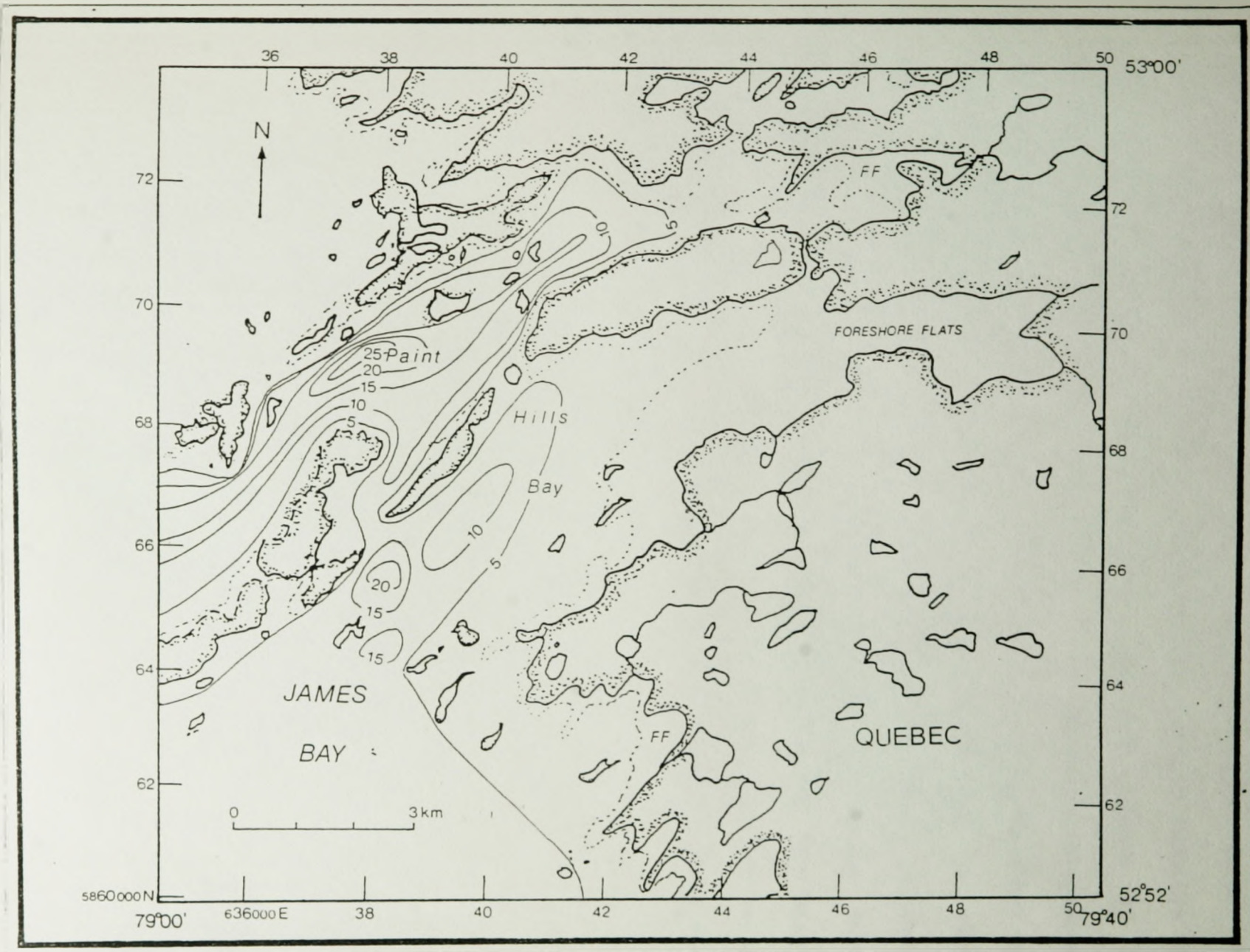
Figure 9: Bathymetry map of Paint Hills Bay, in accordance with
depth soundings from Field Sheet 3792. (5 metre
contour interval)

shallow areas of the foreshore flats.   Plates 9 and 10, on the other

hand, show an area in the south west corner of the study area.   This

image,   showing Solomon's Temple island series, clearly displays signs

of bottom topography.   Four transects, outlined in Plate 5, were

graphed according to pixel counts values.   The profiles, displayed in

Figure 10,   show that areas over apparent bars give higher pixel count

values of 58 and 59.   The counts jump greatly when land is encoun-

tered, as in transects B and D.   These transects, then, follow the

suspected trend of increasing pixel counts with decreasing depths.

Unfortunately no measured bathymetry data are given for this area of

Field Sheet 3792 and, therefore, no corresponding depths can be esta-

blished.   Nevertheless, these transects are encouraging, since bottom

topography is clearly evident
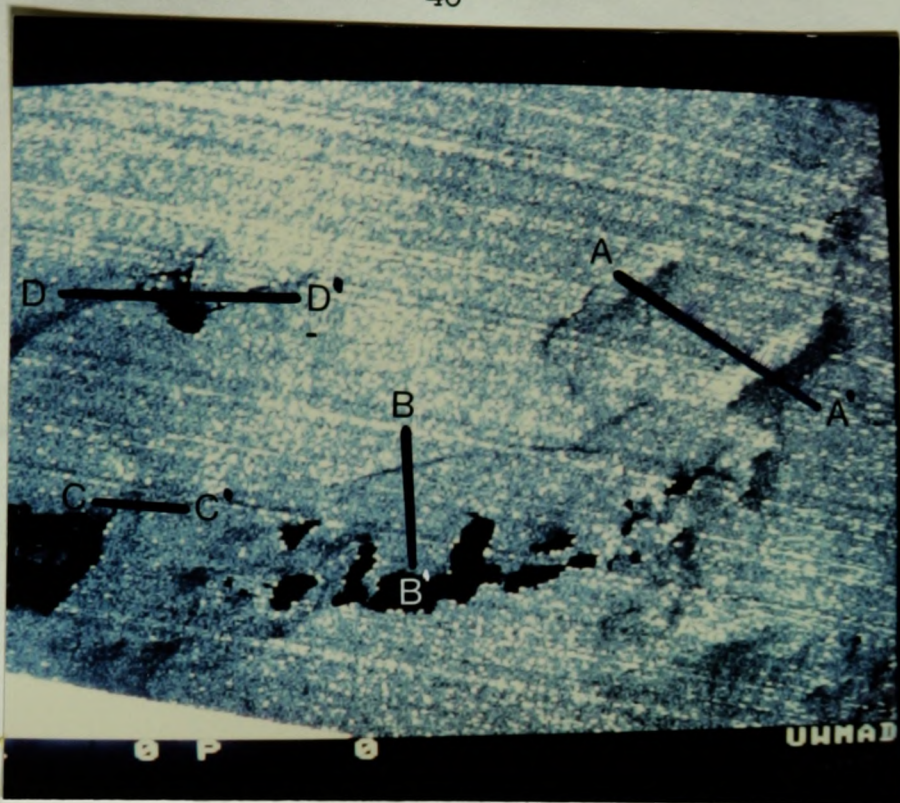
Plate 9:   Calculated water depth image of Solomon's
           Temple islands, south-west corner of the
           study area. Shown are four transects over
           apparent bars for which pixel value read-
           ings were taken.

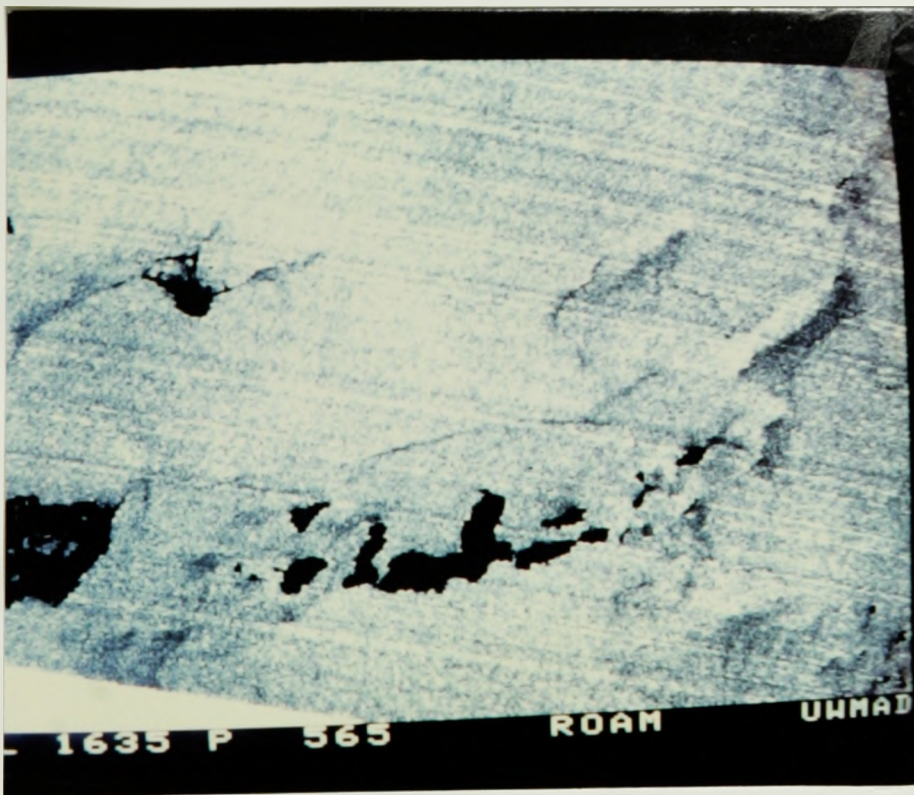

Plate 10: Calculated water depth image of Solomon's
           Temple island series, south-west corner
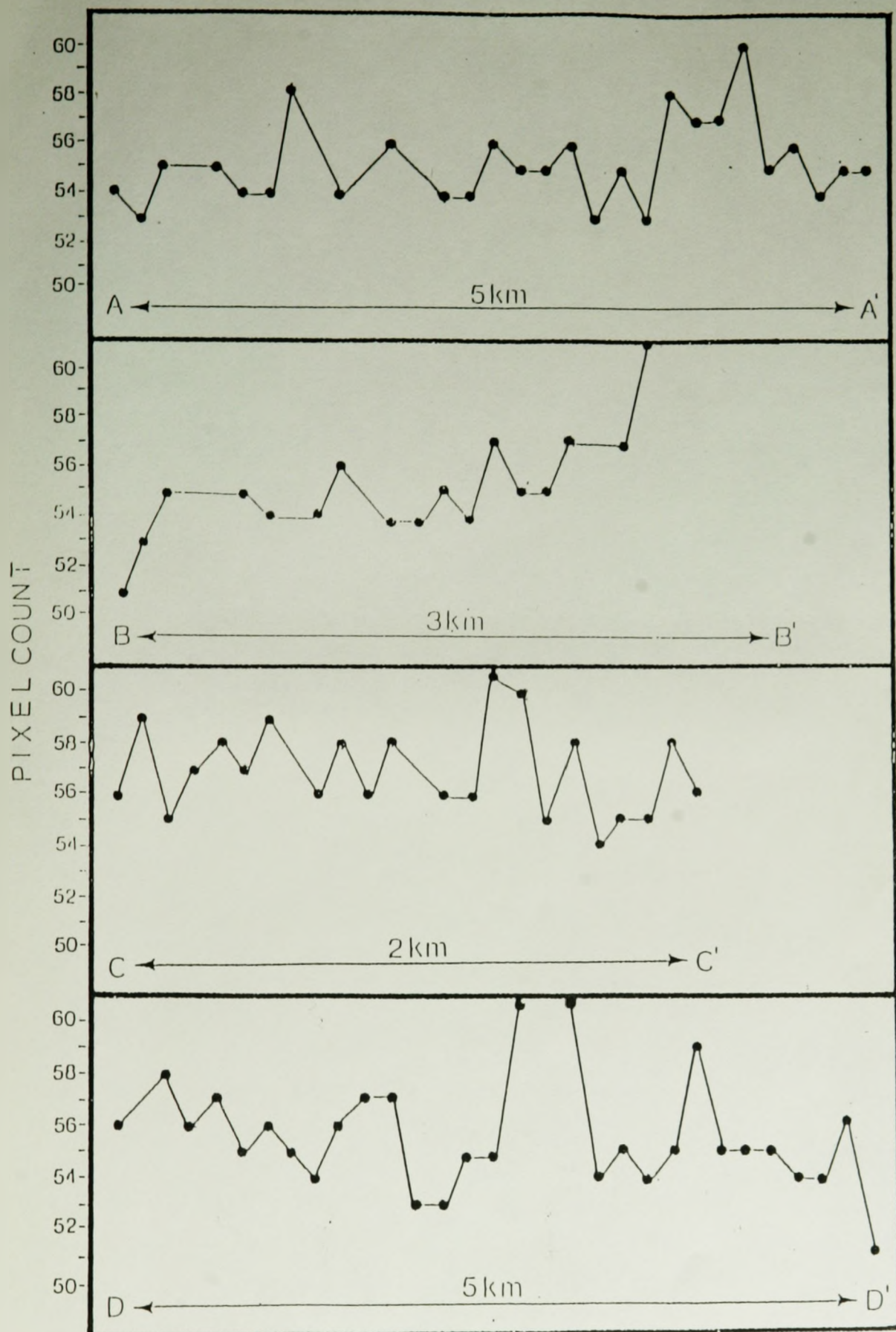   of the study area, for Trial 6.

Figure 10: Profiles of bar transects shown in Plate 9. These transects are graphed according to pixel value readings taken systematically along the transect.

5.   DISCUSSION

    The biggest question arising from the results derives from the fact that the shallow foreshore flats give deep water values. A pixel dump of the light area in the north east corner of the image confirms that count values are ranging from 50 to 53. Thus, values that should be corresponding to deep water are showing up in the very shallow areas. This explains the correlation increase when a Vs of 53 is used, since all counts lower than 53 would give zero depths (see Table 2) and therefore correlate better with the shallow depths. Why this is happening cannot be explained with any large degree of confidence, since the physical characteristics of the area are not well known. Nonetheless, one might form some conjecture as to the reason. Figure 11 shows the distribution of eel grass in 1973. It can be seen that eel grass covers the shores just north of the study site. Perhaps over the last 13 years, this eel grass has migrated southward. If this were the case, it could explain the questionable results. Vege-tation, although it reflects light in the green band of the visible spectrum, absorbs light reaching into the blue wavelengths. Therefore, light would have a tendency not to be reflected from the shallow waters where eel grass may be growing, but instead, would be absorbed, giving a false impression of deep water.

    Even if this were the case, the results of this study are still inadequate. The fact that the pixel counts cover such a narrow range for the waterbody, creates the problems associated with a limited data set. With such a small range, one count value must account for
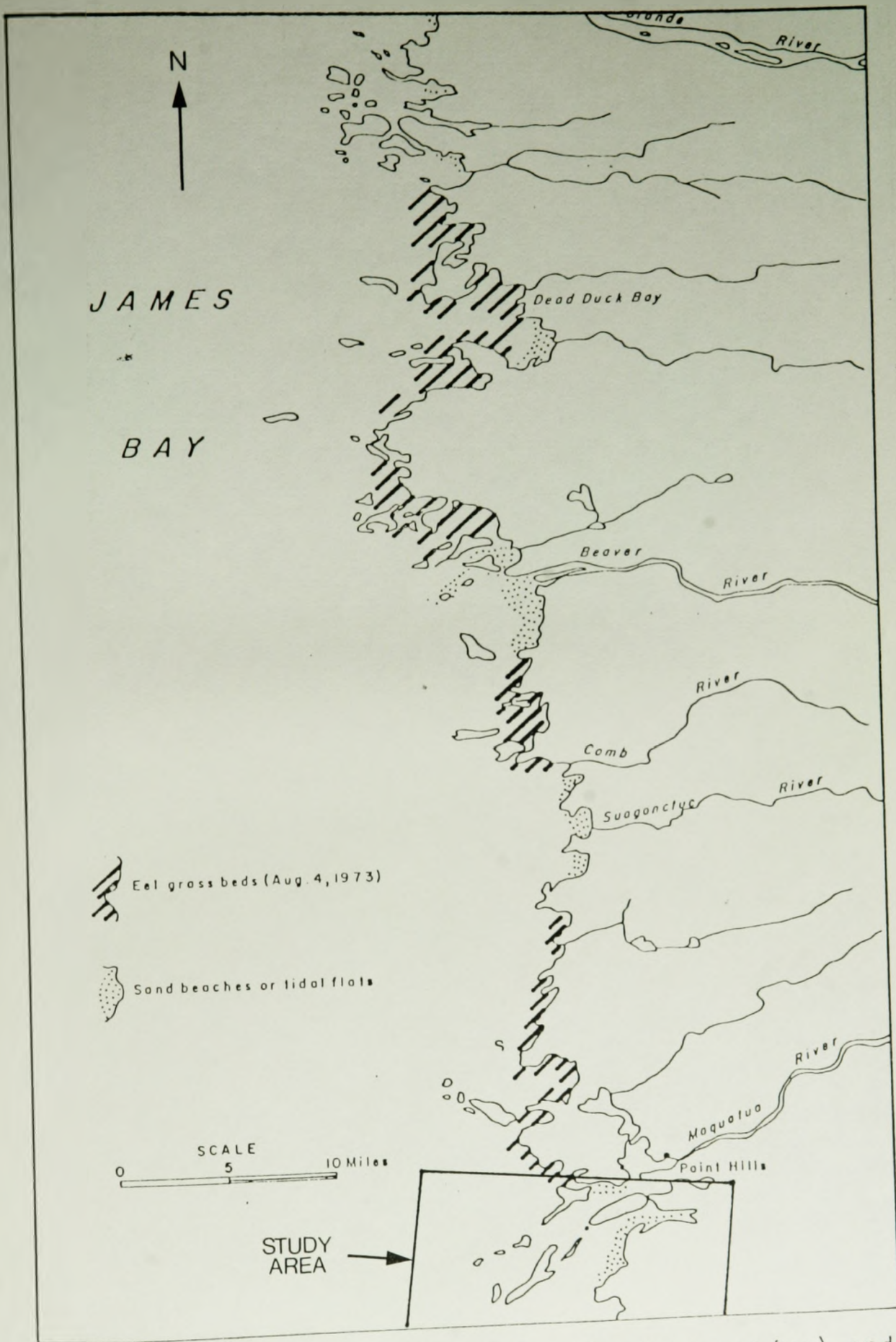
Figure:11 Distribution of eel grass (*Zostera marina*) and tidal flats or beaches along east coast of James Bay.

too varied a depth to be accurate. Figure 7 shows the range in measured depth values for the digital counts found in the data set. One can readily see that the range in measured depths is simply too large to ever be accurate. A count of 54, for example, has a range in depths from 6.6 m to 25 m. This range is too great to create a significant correlation between measured and calculated depths, regardless of the parameters entered into the equation. It is this limited range of pixel values for the water body, that creates the most severe and irreversible problem with the study results. The most likely explanation for this narrow range, is probably due to poor reflectancy of a mud bottom type. Bottom reflectance, it has been shown, is a major parameter in the Polcyn model and therefore a major component of water depth determination. A poor reflectance, of less than 10%, may simply not suffice to give adequate amount of reflected light back to the satellite. Consequently the range in counts becomes too limited.

5.1 RECOMMENDATIONS

If this study were to be carried out again, in an attempt to achieve better results, various changes would have to be made. First, the bottom sediments of the study site would have to have a higher albedo value, such as that associated with a sand bottom. Second, the water would have to be known to be relatively clear, to allow for maximum penetration of light. Thirdly, the sea bottom should be quite flat with gradual changes in depth, so that a good reflectance average

would be given for the 30 m pixel size.   This may not be true of this study site which is rugged and has quite variable depths.   Since most of these conditions cannot be fulfilled for an area such as James Bay, and since fulfillment of these conditions would defeat the whole purpose of this study, it must be concluded that Landsat Thematic Mapper digital imagery cannot be used to accurately determine water depths for an area of James Bay.

6.   SUMMARY AND CONCLUSION

A Landsat Thematic Mapper digital image of a 30 km^2 area on the eastern coast of James Bay, in the vicinity of Paint Hills, was analysed in an attempt to accurately determine coastal water depths. Using a maximum liklihood classification method and a water depth determination method, based on a model developed by Polcyn (1976), computed water depths were compared to actual measured bathymetry. Although some bottom topography was delineated, no accurate results could be assumed from this study.

Classifications showed no visual correlations to measured water depths, since the water body failed to reveal any natural classes. The Polcyn water depth equation proved useless on the given data set, since reflectance values, given in pixel counts, covered too narrow a range to allow for accurate water depth estimates. Calculated water depth imagery showed some visual representation of bottom topgraphy, but, vast annomolies were revealed in the near shore zones of the study site.

This study has thoroughly examined the feasability of the utilization of Landsat TM digital imagery for water depth determination. It has been determined that water topography can, indeed, be delineated. However, with few positive results, it must be concluded that TM data is not a recommended means of bathymetric study in the James Bay area.

REFERENCES

Brown, W.L., F.C. Polcyn, A.N. Sellman, and S.R. Stewart, 1971. Water depth measurements by wave refraction and multispectral techniques; Report No. 31650-31-T, Willow Run Laboratories, Ann Arbor.

Bukata, R.P., J.H. Jerome, A.G.Bobba, and G.P. Harris, 1976. The application of Landdsat-1 digital data to a study of coastal hydrography; C.C.I.W unpub. report, pp. 331-348.

Bullard, R.K., 1983. Land into sea does not go; in, Remote Sensing Applications in Marine Science and Tchnology, D. Reidel Pub. Co. pp. 359-371.

Bullard, R.K., 1983. Detection of marine contours form Landsat film and tape; in, Remote Sensing Applications in Marine Science and Technology, D. Reidel Pub. Co., pp. 373-381.

Dionne, J.C., 1980. An outline of the eastern James Bay coastal environments; in The Coastline of Canada, S.B. McCaan, editor; Geological Survey of Canada, Paper 80-10, p. 311-338

Dionne, J.C., 1986. Personal consultation, August 3, 1986.

Dohler, G.C., 1968. Tides and currents; in Science, History and Hudson Bay, C.S. Beals, ed.; Ottawa, Department of Energy, Mines and Resources, V.2, p. 824-837.

Godin, G., 1972. The tides in James Bay; Environment Canada, Marine Sciences Branch, Manuscript Report Services, 24, p. 97-142.

Godin, G., 1974. The tides in eastern and western James Bay; Arctic. V.27, No.2, p. 104-110.

Guttmen, A., 1968. Extinction coefficient measurements of clear atmospheres and thin cirrus clouds. Appleid Optics, v. 7, no. 12, pp. 2377-2381.

Jain, S.C., H.H. Zwick, and R.A. Neville, 1981. Passive bathymetry with airborne multispectral scanner; 7th Canadian Symposium on Remote Sensing of Environment, Ann Arbor, 1981, pp. 10.

Kapoor, D.C., 1976. International cooperation in hydrography; International Hydrographic Review, LIII (2), pp. 7-15.

Kim, H.H. and G. Linebaugh, 1985. Early evaluation of Thematic Mapper data for caostal process studies; Adv. Space Res., V.5, No.5, pp. 21-29..pa

Lohmann, P., 1985. The determination of water depth using multispectral data and factor analysis; International Symposium on Photogrammetry and Remote Sensing of the Sea, Sept. 6-8, 1985, pp. 266-276.

Lyzenga, D.R., C.T., Wezernak, and F.C. Polcyn, 1976. Spectral band positioning for purposes of bathymetry and mapping bottom features form satellite altitudes, NASA - Technical Report - 115300-5-T, pp.61.

Meagher, L.J, Ruffman, A. and J.M. Stewart, 1976. Marine geological data synthesis. James Bay; Geological Survey of Canada, Open File 497, 2 volumes, pp.561.

O'Neill, N.T., A.R. Kalinauskas, J.D. Dunlop, A.B. Hollinger, H. Edel, M. Casey, and J. Gibson, 1985. Bathymetric analysis of geometrically corrected imagery data collected using two dimensional imagery; Moniteq Report No. 637-26, pp. 7.

Paltridge, G.W. and C.M.R. Platt, 1976. Radiative processes in meteorology and climatology. Developments in Atmosheric Science 5. Elsvier, Amsterdam. pp. 318.

Polcyn, F.C. and D.R. Lyzenga, 1973. Updating coastal and navigational charts using ERTS-1 data; 3rd Earth Resources Technology Satellite Symposium, NASA SP-351, pp. 1333-1346.

Polcyn, F.C. and D.R. Lyzenga, 1975. Remote bathymetry and shoal detection with ERTS; Report No. 193300-51-F, Environmental Research Institute of Michigan, Ann Arbor.

Polcyn, F.C., 1976 Final report on NASA/Cousteau ocean bathymetry experiment - Remote bathymetry using high hain Landsat data; NASA-CR-ERIM-118500-1-F, pp. 132.

Richardson, K., 1985. Thematic Mapper (TM) analysis of Nantucket's nearshore marine environment; OCEANS' 85, MTS/IEEE, pp. 11.

Smith, R.C., and K.S. Baker, 1978. Optical classification of natural water. Limno. Oceanogr., V.23, No.2, pp. 260-267.

U.S. Navy, 1968. Oceanographic Atlas of the North Atlantic Ocean, Section 3: Ice. Washington, D.C.: Naval Ocanographic Office (Defense Department Publication no. 700).

Weidmark, W.C., S.C. Jain, H.H. Zwick, and J.R. Miller, 1981. Passive bathymetric measurements in the Bruce Peninsula region of Ontario; 15th International Symposium on Remote Sensing of the Environment, Ann Arbor, 1981, pp. 10.

APPENDIX

APPENDIX

TABLE 1

Table 1. Spectral attenuation coefficient, K_u (m^{-1}) and K_{x2}(m^{-1}), and spectral values of the specific attenuation coefficients $k_1(\lambda)$ and $k_2(\lambda)$.

λ[nm]	$K_w(\lambda)$	$K_{x2}(\lambda)$	$k_1(\lambda)$	$k_2(\lambda)$	$\Lambda K(\lambda)$
350	0.059	0.177	0.249	0.066	0.024
355	0.055	0.177	0.249	0.066	0.024
360	0.051	0.177	0.249	0.066	0.024
365	0.045	0.178	0.248	0.063	0.028
370	0.044	0.179	0.245	0.061	0.020
375	0.043	0.179	0.240	0.058	0.013
380	0.040	0.179	0.237	0.055	0.014
385	0.036	0.179	0.232	0.053	0.000
390	0.031	0.177	0.227	0.051	0.009
395	0.029	0.175	0.223	0.050	0.009
400	0.027	0.172	0.216	0.049	0.025
405	0.026	0.167	0.210	0.048	0.027
410	0.025	0.162	0.205	0.047	0.024
415	0.024	0.156	0.200	0.046	0.013
420	0.024	0.150	0.194	0.045	0.005
425	0.023	0.145	0.187	0.044	0.010
430	0.022	0.137	0.181	0.042	0.006
435	0.022	0.132	0.175	0.041	0.007
440	0.022	0.125	0.168	0.039	0.021
445	0.023	0.121	0.163	0.038	0.022
450	0.023	0.116	0.158	0.037	0.030
455	0.023	0.112	0.150	0.036	0.013
460	0.023	0.110	0.146	0.034	0.011
465	0.023	0.104	0.141	0.033	0.029
470	0.023	0.100	0.135	0.031	0.027
475	0.022	0.095	0.130	0.030	0.038
480	0.022	0.091	0.125	0.029	0.034
485	0.024	0.087	0.120	0.027	0.042
490	0.025	0.084	0.115	0.026	0.043
495	0.027	0.080	0.110	0.025	0.045
500	0.029	0.077	0.105	0.024	0.035
505	0.033	0.074	0.102	0.022	0.056
510	0.037	0.071	0.096	0.021	0.039
515	0.043	0.069	0.093	0.020	0.045
520	0.048	0.066	0.088	0.019	0.033
525	0.050	0.064	0.085	0.017	0.047
530	0.050	0.061	0.084	0.016	0.085
535	0.052	0.060	0.080	0.015	0.062
540	0.055	0.059	0.076	0.014	0.042
545	0.059	0.056	0.073	0.013	0.049
550	0.063	0.055	0.070	0.012	0.044
555	0.067	0.054	0.070	0.011	0.070
560	0.071	0.053	0.070	0.011	0.087
565	0.074	0.052	0.071	0.010	0.120
570	0.077	0.053	0.072	0.009	0.133
575	0.082	0.054	0.074	0.009	0.154
580	0.088	0.056	0.077	0.008	0.160
585	0.099	0.059	0.085	0.008	0.213
590	0.107	0.066	0.095	0.007	0.223
595	0.121	0.091	0.110	0.007	0.105
600	0.131	0.131	0.125	0.007	0.106
605	0.146	0.150	0.148	0.007	0.060
610	0.170	0.159	0.168	0.007	0.014
615	0.188	0.165	0.184	0.006	0.069
620	0.212	0.167	0.195	0.006	0.109
625	0.244	0.169	0.205	0.006	0.146
630	0.277	0.161	0.213	0.006	0.213
635	0.300	0.137	0.222	0.007	0.350
640	0.327	0.117	0.227	0.007	0.449
645	0.339	0.095	0.231	0.008	0.554
650	0.336	0.061	0.225	0.009	0.686
655	0.337	0.037	0.205	0.011	0.765
660	0.390	0.015	0.180	0.012	0.850
665	0.425	0.002	0.156	0.014	0.896
670	0.460	0.0	0.118	0.015	0.873
675	0.485	0.0	0.088	0.016	0.823
680	0.510	0.0	0.068	0.015	0.779
685	0.540	0.0	0.045	0.014	0.693
690	0.570	0.0	0.028	0.011	0.596
695	0.600	0.0	0.015	0.008	0.460
700	0.630	0.0	0.008	0.004	0.450

(Smith and Baker, 1978)

APPENDIX

FIGURE 1
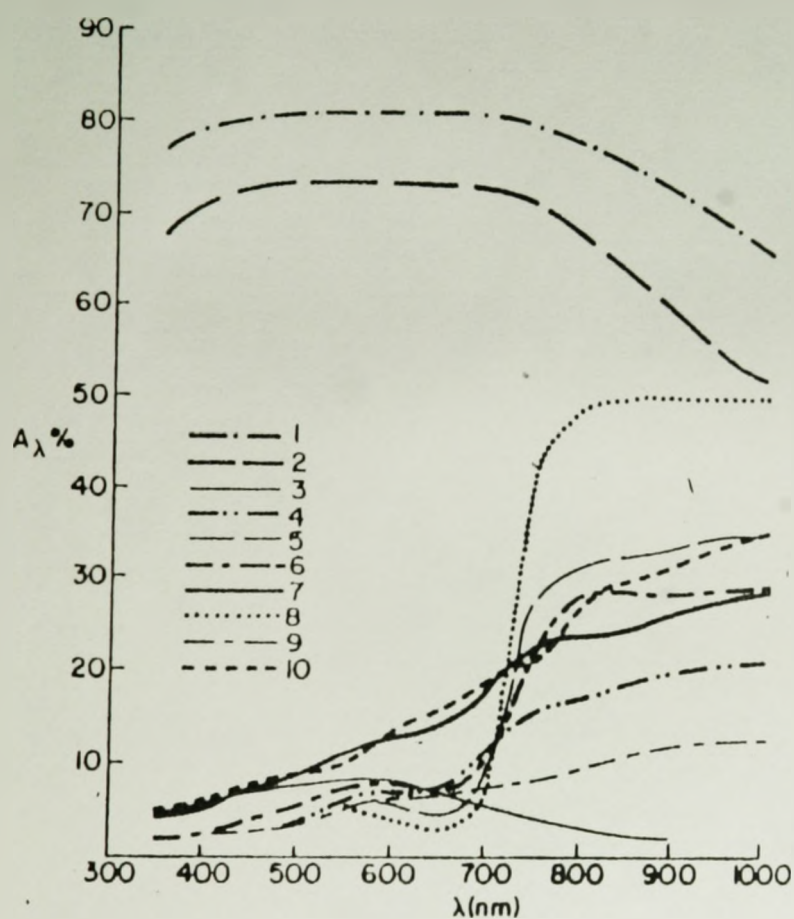
Spectral albedo of different natural underlying surfaces at various solar elevations γ. 1 = snow with ice crust, $\gamma = 38°$; 2 = large-grained wet snow, $\gamma = 37°$; 3 = water surface of a lake, $\gamma = 56°$; 4 = soil after thawed snow, $\gamma = 24°30'$; 5 = silage corn, $\gamma = 54°$; 6 = tall greencorn, $\gamma = 56°$; 7 = yellow corn, $\gamma = 46°$; 8 = sudan grass, $\gamma = 52°$; 9 = chernozem, $\gamma = 40°$; 10 = stubble of cereals, $\gamma = 35°$.
(Paltridge and Platt, 1976)
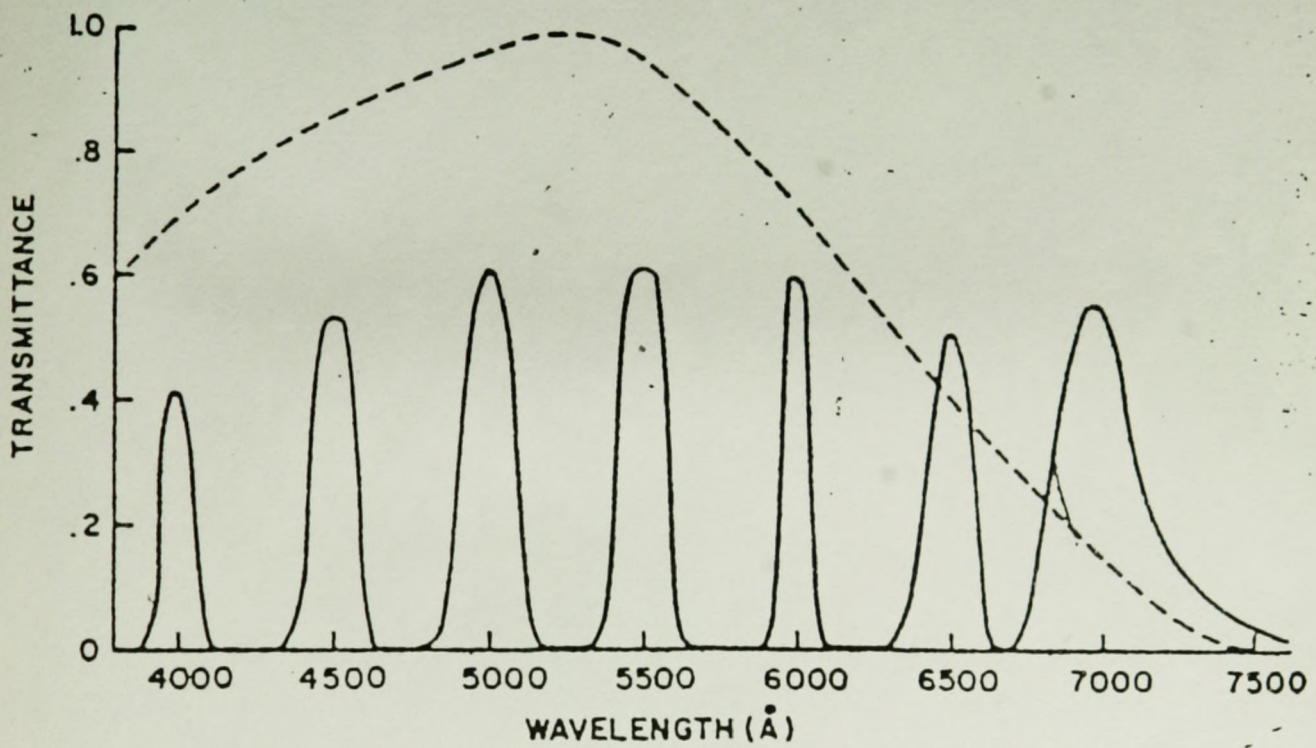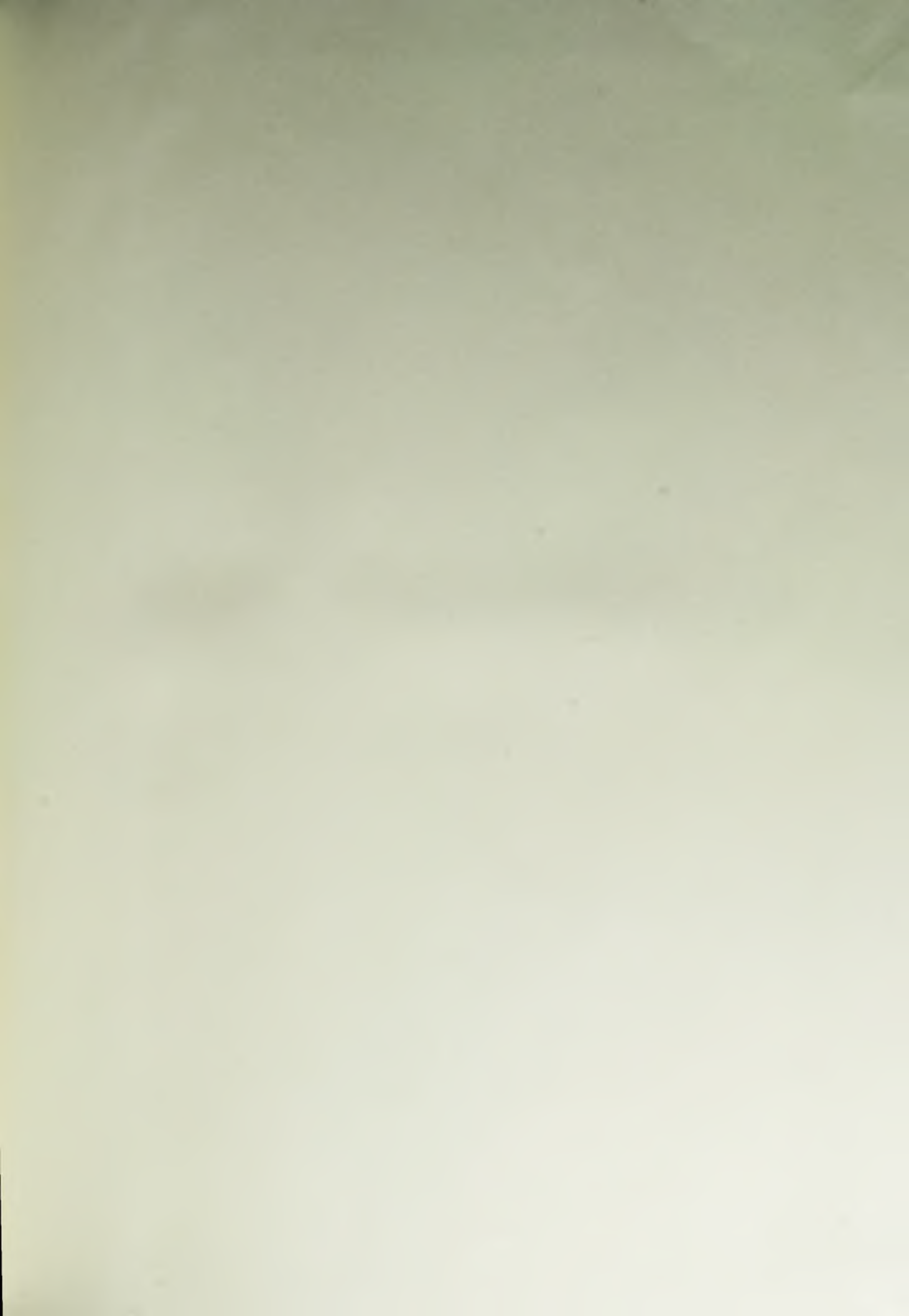
APPENDIX

FIGURE 2

Fig. 1.   Spectral transmission curves for bandpass filters used with radiometer whose normalized spectral response is shown by dashed curve.
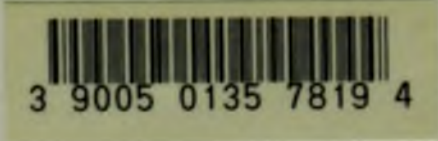
(Guttman, 1968)

53

DIGITAL PIXEL COUNTS AND
CORRESPONDING MEASURED WATER DEPTHS

Water Depths in meters

COUNT	50	51	52	53	54	55	56	57	58	59	60	77	81
1	2.6	--	2.0	3.6	6.6	8.4	8.8	5.8	3.6	--	5.2	17.8	2.4
2				3.6	7.4	8.8	10.0	6.8	14.2				
3				4.6	7.8	9.4	10.4						
4				5.6	8.2	9.6	11.0						
5				5.6	8.4	9.6	11.2						
6				10.4	10.0	12.4	20.4						
7				13.6	11.8	13.6							
8				15.6	13.6	13.6							
9					14.2	14.2							
10					16.4	16.0							
11					18.2	17.0							
12					19.0	17.4							
13					19.8								
14					20.6								
15					23.6								
16					25.0								
MEAN	2.6	--	2.0	7.8	14.4	12.5	12.0	6.3	8.9	--	5.2	17.8	2.4
RANGE	"		"	12.0	18.4	9.0	11.6	1.0	10.6		"	"	
ST.DEV				4.7	6.1	3.3	4.2	0.7	7.5				

Thesis
G
970851